

Warming the MATRIX: Uncertainty and heterogeneity in climate change impacts and policy targets in the Euro Area[☆]

Davide Bazzana^{a,b,*}, Massimiliano Rizzati^{a,b}, Emanuele Ciola^{a,b}, Enrico Turco^{a,c}, Sergio Vergalli^{a,b}

^a *Fondazione Eni Enrico Mattei, Corso Magenta 63, Milano, 20123, MI, Italy*

^b *Department of Economics and Management, Università degli Studi di Brescia, Via San Faustino 74/B, Brescia, 25122, BS, Italy*

^c *The Complexity Lab in Economics, Department of Economics and Finance, Catholic University of Milan, Via Necchi 5, Milano, 20123, MI, Italy*

ARTICLE INFO

JEL classification:

C63
Q52
Q58

Keywords:

Energy sector
Agent-based models
Macroeconomic dynamics
Climate change
Climate policy
Emission abatement

ABSTRACT

This paper explores the potential impacts of climate change and mitigation policies in the Euro Area, considering the uncertainty and heterogeneity in both climate and economic systems. Using the MATRIX model, a multi-sector and multi-agent macroeconomic model, we simulate various climate scenarios by employing different carbon cycle models, damage functions, and marginal abatement curves found in the literature. We find that heterogeneous climate damages amplify both the magnitude and the volatility of GDP losses associated with global warming. By the end of the century, we estimate that assuming homogeneous shocks may underestimate the effects of climate change on aggregate output by up to one-third. Moreover, we find that the speed and feasibility of a low-carbon transition crucially depend on (i) the ambition in emission reduction targets set by the policymaker, which determine the level of a carbon tax, and (ii) the rate of technological progress, which influences the shape of the abatement cost curve.

1. Introduction

Climate change is considered one of the most pressing challenges of our time. Its impacts are not only environmental but also economic and social, affecting all sectors of society in different ways. However, understanding the economic effects of climate change is a complex task due to the presence of uncertainty and heterogeneity in both climate and economic systems (Brown and Kroll, 2017). Climate uncertainty stems from the unpredictable and long-term consequence of climate change, caused, on the one hand, by the uncertain evolution of CO₂ emissions resulting from human activity and, on the other hand, by an incomplete understanding of Earth's systems and their interactions. Economic heterogeneity arises from different characteristics, preferences, and behaviors of various agents such as households, firms, and governments. In a complex evolving economy, heterogeneous agents adapt to a changing environment and interact in decentralized markets using simple heuristics due to limited information and computational

abilities (Tversky and Kahneman, 1974; Gigerenzer, 2002; Dosi et al., 2020). That can lead to coordination failures and market feedback loops resulting in economic uncertainty that ultimately affects the climate system.¹ At the same time, evidence indicates that climate damages are heterogeneously distributed, between and within countries, among agents operating in different areas and sectors that are not equally exposed to extreme weather events (Schmidt et al., 2012; Palagi et al., 2022).

The goal of this paper is to assess the economic impacts of climate change and mitigation policies, taking into account the role of uncertainty and heterogeneity in climate and economic systems. To do that, we propose a climate extension of the Multi-Agent model for Transition Risks (MATRIX) described in Ciola et al. (2023) and Turco et al. (2023).

The extended MATRIX model is an agent-based integrated assessment model that combines an economic and a climate module. The former develops a multi-sector and multi-agent macroeconomic replica

[☆] The authors would like to thank the editor, two anonymous reviewers, and the participants at the 11th IAERE annual conference, 26th WEHIA annual workshop, 28th EAERE annual conference, 29th CEF international conference, ECEMP 2023 annual conference, and 16th IAMC conference for useful comments.

* Corresponding author at: Department of Economics and Management, Università degli Studi di Brescia, Via San Faustino 74/B, Brescia, 25122, BS, Italy.

E-mail addresses: davide.bazzana@unibs.it (D. Bazzana), massimiliano.rizzati@feem.it (M. Rizzati), emanuele.ciola@unibs.it (E. Ciola), enricomaria.turco@unicatt.it (E. Turco), sergio.vergalli@unibs.it (S. Vergalli).

¹ For the sake of example, in late 2021, higher natural gas prices due to the market imbalances resulting from the post-Covid recovery and subsequent global energy crisis, further exacerbated by the Russia-Ukraine war, led many countries to slow down the process of phasing out coal, with evident adverse effects on the environment.

of the Euro Area (EA). It considers a diverse set of agents belonging to different sectors, such as households, corporates, banks, and public entities interacting in decentralized markets. Private companies comprise energy, capital, and consumption goods firms, all of which generate CO₂ emissions through the consumption of fossil fuels. The climate module includes a carbon cycle and a climate damage function. The carbon cycle converts the model-generated emissions of the EA and the exogenous emissions from the rest of the world into atmospheric concentrations of CO₂, ultimately leading to an increase in the average global temperature. The damage function maps the temperature increase into economic losses that hit firms' production capacity. To mitigate the detrimental effects of global warming, the government can implement a carbon tax, adjusting its level as a function of the gap between targeted and actual emissions reduction. The introduction of the carbon tax, which represents an implicit price of emitting, motivates firms to invest in cost-effective abatement technologies, whose abatement potential increases with their costs, following the standard Marginal Abatement Cost (MAC) curve approach.

To comprehensively assess the impacts of climate change and mitigation policies under uncertainty and heterogeneity, we leverage the granularity and flexibility of the agent-based modeling by testing various carbon cycle models, damage functions, and MAC curves found in the literature. We also consider different types of climate damage depending on whether they are distributed homogeneously or heterogeneously across agents. This approach enables us to address the dual dimension of uncertainty in the economic and policy analysis of climate change: firstly, the bottom-up approach of the agent-based framework accounts for uncertainty in aggregate climate and economic outcomes resulting from the casual interactions of heterogeneous agents in decentralized markets; secondly, the comparison of various climate models in the literature addresses the uncertainty in modeling assumptions regarding functional forms and parameter specification that may impact results.

Simulation results show that climate change will cause average GDP losses to grow with rising temperatures, particularly when considering heterogeneous climate shocks. Specifically, under homogeneous climate damages, the average realized losses at the end of the century increase from 1.2% under a low-temperature scenario (+2 °C) to 3.7% under a high-temperature one (+3.8 °C), that is consistent with existing studies in the standard Integrated Assessment Models (IAMs) literature.² In contrast, when accounting for heterogeneous climate damages, average GDP losses surge by 50% compared to the homogeneous scenarios, amounting to 1.6% and 5.3% in the coldest and hottest projections. In the most extreme scenario, average losses peak at 9.1%, also revealing a more skewed distribution that suggests a higher likelihood of catastrophic events.³ Therefore, in the presence of heterogeneous climate shocks, rising temperature affects both the magnitude and the volatility of economic losses resulting from climate change.

Further analysis of climate impacts on other macroeconomic variables demonstrates that homogeneous climate damages act similarly to conventional supply shocks. That leads to higher prices, lower real wages, and reduced employment. Conversely, heterogeneous climate shocks cause a decline in output and employment, accompanied by falling prices and real wages, similar to a supply-induced demand shock (Guerrieri et al., 2022; Kharroubi and Smets, 2023). That is because coordination failures arising from decentralized market interactions are exacerbated by heterogeneous climate shocks, resulting in

² For example, DICE 1992 estimates a climate damage of 1.5% for a raise in temperatures of +3.2 °C by 2100, whereas the GDP losses due to an increase of +4.3 °C are equal to 4.3% in DICE 2016 (see Nordhaus, 2018).

³ These results can be compared with Lamperti et al. (2018) who estimate an increase of +4.5 °C by 2100, which may produce GDP losses ranging from 1.1% to 84.9% depending on the transmission channel under consideration.

disordered cascading effects on the economy. In contrast, the economy can absorb more quickly homogeneous climate shocks since all agents react similarly to the same amount of economic losses, leading to more efficient coordination. That underscores the limits of standard IAMs founded on the representative agent hypothesis, which run the danger of underestimating the economic impact of climate change (Farmer et al., 2015; Balint et al., 2017).

The analysis of climate policy shows that a higher level of carbon tax is necessary to achieve stricter emission reduction targets. In particular, to achieve a 75% reduction in CO₂ emissions by the end of the century, a value between 110 and 210 euro per ton of CO₂ (EUR/tCO₂) is required, in line with existing studies (see Clapp et al., 2009; Hintermayer et al., 2020; Calvin et al., 2023). However, the pace and possibility of achieving these targets depend crucially on the rate of technological progress, as reflected in the shape of cost abatement curves. Specifically, without abatement options, it would be possible to reduce carbon emissions only by 25% for a given level of the carbon tax because of the limited substitutability of fossil fuel with other factors. High initial abatement costs can delay (or, in extreme cases, prevent) the adoption of less polluting production techniques, thus leading firms to reduce the consumption of fossil fuels in the face of rising emission price or, to some extent, substitute them with other factors. Finally, our analysis reveals that the transition path towards the desired target exhibits a non-linear behavior. That is due to time lags between policy updates and abatement technology adoption, which can cause the carbon tax to overshoot the desired level. As a result, in line with Foramitti et al. (2021b), the government should avoid revising the carbon tax too frequently. That will help maintain a credible commitment and allow the system to respond smoothly to any policy change.

This paper expands the climate economic literature in three distinct ways. First, we contribute to the integrated assessment literature on how uncertainty affects economic analyses of climate change and policy. The standard approach relies upon IAMs to analyze the complex interactions between the economy and the environment and assess the costs and benefits of different policy interventions to mitigate climate change. Despite the significant progress made in IAMs since the pioneering work of Nordhaus (1991), criticisms regarding their ability to accurately account for the role of uncertainty and heterogeneity in shaping climate policy persist (Pindyck, 2013; Farmer et al., 2015; Savin et al., 2023).⁴ In contrast, we employ an agent-based IAM framework, in line with Lamperti et al. (2018), Czupryna et al. (2020) and Safarzyńska and van den Bergh (2022). By simulating the economy as a complex adaptive system, the agent-based approach allows capturing the endogenous sources of uncertainty due to the presence of agent heterogeneity, bounded rationality, and decentralized market interactions without resorting to exogenous stochastic processes meant to internalize the volatility in economic and climate variables, e.g., through geometric Brownian motion. Hence, the agent-based method enables us to account for the inherent uncertainty in the functioning of climate-economic systems. Additionally, to control for the epistemic uncertainty brought on by the application of discretionary modeling assumptions, we simulate alternative scenarios using various specifications of each climate module under consideration (i.e., carbon cycle, damage function, MAC curve).

Second, we contribute to the stream of literature assessing the role of heterogeneity in evaluating climate impacts (Schmidt et al., 2012; Brown and Kroll, 2017). Despite the growing evidence on the importance of heterogeneous effects of climate damage, theoretical exploration of these elements using a modeling method has received

⁴ Although several studies have attempted to incorporate uncertainty in the climate system through stochastic shocks and tipping points that may lead to catastrophic outcomes (Weitzman, 2012; Dietz and Stern, 2015), the role of economic uncertainty has largely been overlooked in this approach.

little attention. The representative agent hypothesis in standard IAMs allows for analyzing the diverse climate impacts between countries (regional inequality) but not among individuals living in the same area (socio-economic inequality). There are few exceptions in conventional (Dennig et al., 2015) and agent-based literature (Lamperti et al., 2018; Safarzyńska and van den Bergh, 2022).

Third, we add to the growing body of agent-based literature on climate and economic assessment of mitigation policies (Balint et al., 2017; Castro et al., 2020). Based on the DSK model, Lamperti et al. (2020) compare the effects of market-based versus performance-based climate policies on the direction of technical change and the prevention of environmental disasters. They find that command-and-control interventions are superior to market-based ones such as carbon tax or green subsidies, as the former is favored by path dependence and guarantees policy effectiveness irrespective of the timing of their introduction. Foramitti et al. (2021a) compare the performance of emission tax versus permit trading using a one-sector agent-based model, finding that, under the latter arrangement, permit price falls after the successful abatement, leading to higher production levels and resource misallocation.

In this paper, we propose a novel approach to climate policy that involves setting a predetermined emission reduction target and allowing the government to progressively adjust the carbon price based on the gap between desired and actual emissions. Such a target-based policy approach has the following advantages: (i) it allows reproducing the EU's climate goal of reducing its emissions as defined in the "Fit for 55" package; (ii) it prevents the choice of setting arbitrary values for the carbon tax and adjustment steps; (iii) it allows focusing on emission reduction plans in a specific area, such as the EA economy, whereas climate policies based on temperature targets inevitably call for the adoption of global or multi-regional models, or making inferences on the emissions pattern coming from the rest of the world.

In the following, Section 2 describes the overall structure of the MATRIX model, Section 3 presents the calibration procedure, and Section 4 discusses the results of the simulation experiments. Section 5 concludes and states future research directions.

2. Model

The *Multi-Agent model for Transition Risks* – the MATRIX model – (Giola et al., 2023; Turco et al., 2023) is an agent-based stock-flow consistent⁵ macroeconomic model developed to analyze the functioning of real-world economies with a focus on energy production and consumption. Under the assumption of an economic system comprising a multiplicity of heterogeneous agents, the model generates the endogenous dynamics of the simulated economy from their decentralized interactions in different markets. In particular, workers provide labor to energy (E), consumption (C), and capital (K) firms, which employ it with other inputs in a Constant Elasticity of Substitution (CES) production function to supply sector-specific goods. The latter then enter as intermediate production inputs in other sectors (i.e., energy services and capital) or are used for final consumption by households. At the same time, banks collect deposits and provide credit to firms to finance production, the government collects taxes and transfers financial resources to low-income individuals, and the central bank sets the policy rate following an inertial Taylor rule. Lastly, an exogenous fossil fuel producer inelastically supplies a raw energy input at a given price as an additional production factor as in Ponta et al. (2018).⁶

⁵ In other words, it adheres to the accounting principle by which any change in flow variables produces a corresponding variation in stock variables, and each agent's assets represent another agent's liabilities. Appendix A.8 reports the tables describing the aggregate balance sheet and transaction flow matrix.

⁶ We set the price such that the ratio of fossil fuels expenditure over total output is in line with EA data (see Section 3).

Considering that a share of oil and gas production occurs domestically through onshore or offshore activities by energy firms, we assume that fossil rents are redistributed within the economy, partly to energy firms (to account for domestic fossil fuel production), and partly to households in proportion to their wealth.⁷

Fig. 1 provides a visual representation of the overall functioning of the model.

Since the focus of this work is on the economic consequences of climate change and mitigation policies for the EA economy, we employ the European calibrated version of the MATRIX model (Turco et al., 2023) as the Business-as-Usual (BAU) scenario for our analysis. Firms now produce CO₂ emissions through their consumption of fossil fuels but can limit them by investing in a costly Abatement Technology (AbT). At the same time, anthropogenic emissions modify the composition of the atmosphere and the energy balance of the planet, resulting in widespread damages that affect the production capacity of the economic system. Nevertheless, the government can (partially) address this process and incentivize investments in the AbT by imposing a carbon tax on CO₂ emissions. Lastly, we assume that firms' productivity grows following an exogenous path to reproduce the long-term dynamics of the EA economy.

The next sections present a general description of the new features of the model, while Appendices A and B provides additional information on the economic and climate modules.

2.1. Emissions

In the new version of the model, firms contribute to anthropogenic climate change by generating CO₂ emissions through their consumption of fossil fuels. That depends on their specific emission intensities, namely:

$$E_{f,t} = e_{f,t} O_{f,t}, \quad (1)$$

where $E_{f,t}$ are current period emissions of firm f , $e_{f,t}$ is the firm-specific emission intensity,⁸ and $O_{f,t}$ is the consumed quantity of fossil fuels. Accordingly, total emissions are equal to the sum of individual contributions:

$$E_t = \sum_{f=1}^{N^F} E_{f,t}. \quad (2)$$

Nevertheless, since the model represents only the EA economy, those values account for only a portion of the global figure. Therefore, we combine them with a set of simulated Rest Of the World (ROW) emissions, E_t^{ROW} , which we generate following the Stochastic Impacts by Regression on Population, Affluence, and Technology (STIRPAT) framework (Dietz and Rosa, 1994, 1997). In particular, we estimate a vector autoregression model on the log differences of global population, GDP per capita, and emission intensities. Subsequently, we employ the estimated parameters to forecast future emissions by bootstrapping multiple paths to include in the simulated economy.⁹

Lastly, the sum of EA and ROW emissions gives the global figure:

$$E_t^W = E_t + E_t^{ROW}, \quad (3)$$

which we increase by one-third (i.e., +33%) to account for non-CO₂ greenhouse gases (see Montzka et al., 2011).

⁷ As in Turco et al. (2023), this assumption avoids the continuous outflow of monetary resources from the national economy due to the purchase of foreign fossil fuels but correctly replicates the statistical properties of the EA current account, which has been balanced in the past two decades. A similar procedure applies to abatement costs (see Section 2.4 and Appendix A.8).

⁸ We calibrate initial emission intensities e_{f,t^*} to reflect sectoral differences at a reference year t^* and convert model units to real-world values (see Section 3 for details).

⁹ See Appendix B for additional details.

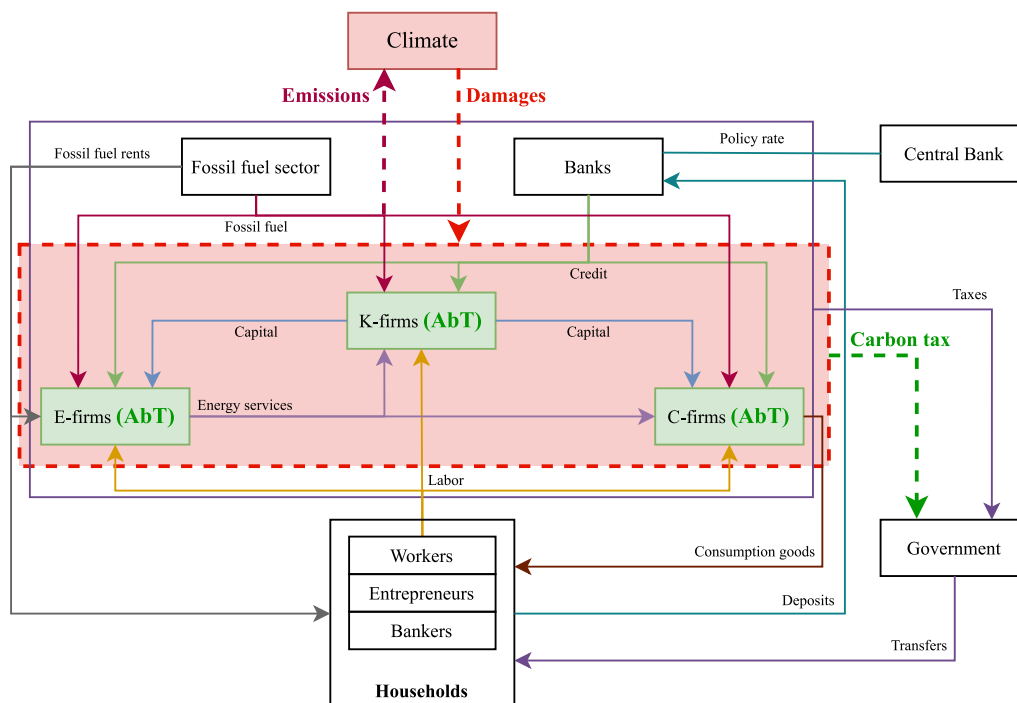


Fig. 1. The MATRIX model and climate extensions (dashed lines and shaded areas).

2.2. Climate module

As stated before, firms contribute to anthropogenic climate change by generating CO₂ emissions through the consumption of fossil fuels. However, there is a huge variety of climate models with varying degrees of complexity in the climate science literature. Accordingly, this work adopts a flexible approach and employs different models to represent the future evolution of the climate and facilitate robustness comparisons.¹⁰

Fig. 2 shows a representative reduced-form carbon cycle with three main boxes: atmosphere, land, and ocean. After flowing into the atmosphere, only a fraction of anthropogenic CO₂ emissions accumulate in it. Indeed, a non-negligible share goes into land and ocean systems because of photosynthesis and the dissolution of carbon in water. Moreover, variations in atmospheric carbon concentrations and temperatures affect the extent of those fluxes by increasing heterotrophic respiration, Net Primary Production (NPP), and air-water carbon exchange. At the same time, the gradual circulation of carbon within boxes (e.g., through thermohaline circulation in the ocean) requires time to reach an equilibrium, thus generating delayed feedback and reflows into the atmosphere. Lastly, the concentration of carbon in the atmosphere determines its radiative forcing, which affects the energy balance of the planet and induces the related change in the global temperature of air and oceans.

Moving from land to its components (vegetation, detritus, and soil) or from ocean to its layers (low and high latitude surface, intermediate or deep), or by defining some intermediate levels of aggregation, the MATRIX model tests a batch of climate modules with increasing degree of complexity. Table 1 shows the alternative forms of the carbon cycle employed in this work with the related sources, while Appendix B provides their detailed description. We start from a simple climate model that does not account for different carbon pools (TCRE) and then move to two comparable climate boxes (DICE-2013R and WITCH) with

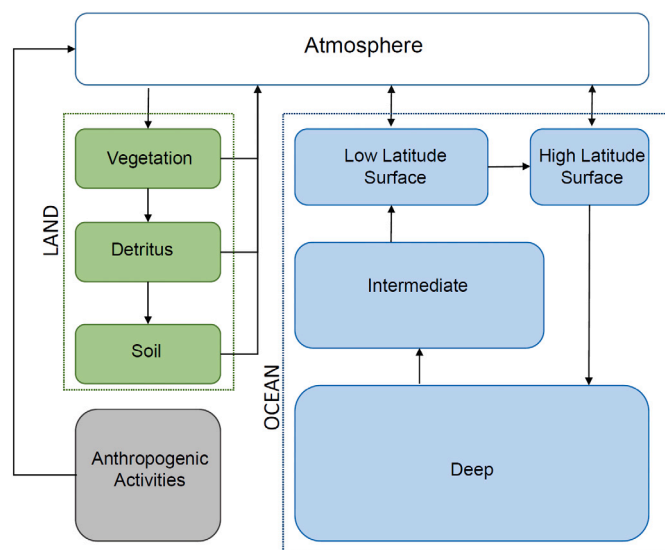


Fig. 2. Representation of the carbon cycle.

3-layers: a one-pool atmosphere plus shallow and deep oceans. Lastly, we test the C-ROADS and HECTOR models. Both expand the carbon cycle by adding a land component with several layers and increasing the complexity of the ocean carbon pool.

2.3. Climate damage

Estimating the economic damages associated with temperature increases is an even more complex and uncertain process, and various factors can affect the accuracy of such estimates. The major challenge is the lack of proper knowledge about the precise shape and parameters of the climate damage function, which describes the relationship between temperature increases and economic damages. As highlighted by Pindyck (2013), its assessment is “the most speculative element of

¹⁰ Burke et al. (2015) report that studies might focus only on a handful of climate models for their projections and suggest using multiple models or an ensemble.

Table 1
Carbon cycles: main boxes.

Name	Boxes	Source
TCRE	Atmosphere	Economides et al. (2018)
DICE-2013R	Atmosphere; surface and deep oceans	Nordhaus (1993a)
WITCH	Atmosphere; surface and deep oceans	Emmerling et al. (2016)
C-ROADS	Atmosphere; vegetation and soil; surface, intermediate and deep oceans	Sterman et al. (2012)
HECTOR	Atmosphere; vegetation, detritus and soil; low and high latitude surface oceans, intermediate and deep oceans	Hartin et al. (2015)

Table 2
Climate damage function.

Name	Average damage	Source
DICE 1991	$CD_t = 0.0133 \left(\frac{\Delta T_t}{3}\right)^2$	Nordhaus (1993b)
RICE 1999	$CD_t = 1 - \frac{1}{1 + 0.001\Delta T_t + 0.049\Delta T_t^2}$	Nordhaus and Boyer (2000)
DICE 2013	$CD_t = 1 - \frac{1}{1 + 0.00267\Delta T_t^2}$	Nordhaus and Sztorc (2013)
DSK 2018	$CD_t = \frac{a_{b,t}}{a_{b,t} + b_{d,t}}$ with $a_{b,t} = \log(1 + \Delta T_t)$ and $b_{d,t} = 100 \frac{\sigma_t^T}{\sigma_t^T}$	Lamperti et al. (2018)

Note: average percentage reduction in labor productivity CD_t , due to a given variation in the global temperature from the preindustrial level ΔT_t . σ_t^T denotes the standard deviation of the global temperature in the last 10 years.

the analysis” (p. 862). To address this challenge, we adopt the same approach used for the climate module and include different climate damage functions to limit the risk of relying on ad-hoc assumptions and control for the uncertainty of economic damage estimates. Moreover, we assess if the presence of heterogeneous climate shocks can amplify their aggregate impact. In particular, we test all functions assuming both homogeneous and heterogeneous damages on the economic agents in the system. In this way, we can provide a more robust evaluation of the economic impacts of climate change.

As shown by Table 2, we employ four standard climate damage functions, which we assume affect production by reducing labor productivity by a percentage CD_t . In DICE 1991, each period’s climate damage takes a simple non-linear functional form based on the current temperature deviation from the preindustrial level (ΔT_t). Its variants (RICE 1999 and DICE 2013) adopt a comparable formulation using a well-known inverse quadratic function, which relates temperature increase to economic losses. Conversely, the DSK 2018 damage function assumes a stochastic process and extracts the realized values from a Beta distribution with parameters $a_{b,t}$ and $b_{d,t}$. The latter, which affect both the mean and the skewness of the distribution, vary over time based on the temperature’s evolution. More precisely, they depend on the difference between the current global temperature and its preindustrial level (ΔT_t) and the growth in temperature volatility (σ_t^T).

Lastly, we model climate damage as both a homogeneous and a heterogeneous shock to labor productivity. In the former case, each agent in the system experiences the same level of economic loss as determined by the damage function CD_t . In the latter case, the damage function represents the average damage in the economy, which is distributed unevenly among agents. In particular, each firm has a probability CD_t of suffering a 100% reduction in labor productivity while it has no losses in the opposite case. As a result, the expected damage experienced by each agent is equal to CD_t .

2.4. Carbon tax and abatement

Carbon tax. The government sets an environmental carbon tax to comply with broader global climate objectives and adaptively adjusts it to reach a desired level of aggregate emissions following a tax adjustment mechanism (Hafstead and Williams, 2020). The reason to exclusively focus on the carbon tax as a climate mitigation policy in this version of the model stems from its prominence in the standard climate-economic literature. In the MATRIX model, if the aggregate emissions

of the economy E_t are above (below) a given threshold \bar{E}^{CA} , then the government increases (reduces) the tax, namely:

$$\tau_t^{CA} = \begin{cases} \tau_{t-1}^{CA} + \epsilon^{CA} & \text{if } E_t > \bar{E}^{CA}, \\ \tau_{t-1}^{CA} - \epsilon^{CA} & \text{otherwise,} \end{cases} \quad (4)$$

where ϵ^{CA} captures the speed of the adjustment, and $\bar{E}^{CA} = (1 - \eta^{CA})E_{t^*}$ is the long-term desired level of emissions, computed in terms of percentage reduction $\eta^{CA} \in [0, 1]$ from a reference year t^* .

The realized carbon tax revenues are then collected at the firm level based on their emissions $E_{f,t}$:

$$TAX_t^{CA} = \tau_t^{CA*} \sum_{f=1}^{N^F} E_{f,t} = \tau_t^{CA} \sum_{f=1}^{N^F} \epsilon_{f,t} P_t^O O_{f,t}, \quad (5)$$

where $\epsilon_{f,t} = e_{f,t}/e_{f^*,t^*}$ are firms’ emission intensities relative to a baseline sector/year $\{f^*, t^*\}$, and $\tau_t^{CA*} = \tau_t^{CA} P_t^O / e_{f^*,t^*}$ is the implicit carbon tax set by the government.¹¹ The additional revenues then enter the government budget, thus updating the public debt B_t to:

$$B_t = (1 + i_{t-1}^{CB}) B_{t-1} + TRA_t - TAX_t^{CA} - TAX_t, \quad (6)$$

where TAX_t is standard tax collection, TRA_t are the transfers to low-income households, and i_{t-1}^{CB} is the risk-free interest rate set by the central bank and paid on government bonds. By increasing the fiscal space, emission revenues allow the government to reduce the standard tax rate and increase the transfers to low-income households. Accordingly, we assume the public sector evenly distributes the additional revenues in those two budget entries.¹²

Abatement. Firms can lower their emissions by investing in a costly AbT provided by an exogenous monopolist.¹³ Following Foramitti et al. (2021a), we assume that the AbT determines a percentage reduction in the emission intensity of firms and involves a number J^{AbT} of identical

¹¹ We model the carbon tax in this way since it allows for its subsequent conversion into real-world monetary units (see Section 3).

¹² See Carraro et al. (1996), Parry and Bento (2000) and Bosello et al. (2001) for analyses on the possible “double dividend” of environmental policies, or Klenert and Mattauch (2016) and Maestre-Andrés et al. (2021) for the redistributive impact of carbon taxes.

¹³ The technology underlying the abatement process is not specified and could involve either an increase in the efficiency or a shift towards less polluting production factors as the model does not explicitly include a green energy input.

steps up to a maximum level \hat{e}^{AbT} . Each step represents a technological advancement for its adopter, characterized by lower emission intensity and a higher MAC. As a result, the investment in a new abatement step depends on the direct comparison between its marginal cost and the carbon tax.

Going into detail, the abatement cost $AC_{f,t}$ depends on the percentage reduction in the emission intensity $\hat{e}_{f,t}$ and the nominal expenditure on fossil fuel $P_t^O O_{f,t}$:¹⁴

$$AC_{f,t} = AC \left(\frac{e_{f,t}^* - e_{f,t}}{e_{f,t}^*} \right) P_t^O O_{f,t} = AC(\hat{e}_{f,t}) P_t^O O_{f,t}. \quad (7)$$

Accordingly, the total costs of emissions are equal to:

$$\begin{aligned} TEC_{f,t} &= \tau_t^{CA} E_{f,t} + AC(\hat{e}_{f,t}) P_t^O O_{f,t} \\ &= [\tau_t^{CA} \varepsilon_{f,t} (1 - \hat{e}_{f,t}) + AC(\hat{e}_{f,t})] P_t^O O_{f,t} \\ &= EC(\hat{e}_{f,t}) P_t^O O_{f,t}, \end{aligned} \quad (8)$$

and each firm has the incentive to invest in an additional abatement step as long as:

$$\frac{\partial EC(\hat{e}_{f,t})}{\partial \hat{e}_{f,t}} < 0 \implies \tau_t^{CA} > \frac{1}{\varepsilon_{f,t}^*} \frac{\partial AC(\hat{e}_{f,t})}{\partial \hat{e}_{f,t}} = \frac{1}{\varepsilon_{f,t}^*} MAC(\hat{e}_{f,t}). \quad (9)$$

As a result, the shape of the MAC curve plays a crucial role in determining the investment decision. Therefore, we control for the uncertainty surrounding this function by considering different functional shapes (see Section 3). Moreover, since adopting new technology may require time, we suppose that firms can update their abatement step with probability θ^{AbT} .

Lastly, since we assume the AbT as a discrete process divided in J^{AbT} identical steps $\left\{ j \frac{\hat{e}^{AbT}}{J^{AbT}} \right\}_{j=0}^{J^{AbT}}$ and given the maximum percentage reduction in the emission intensity \hat{e}^{AbT} , the current abatement costs of a firm f at step $J_{f,t}$ approximates as:

$$AC(\hat{e}_{f,t}) \approx \sum_{j=0}^{J_{f,t}} \frac{\hat{e}^{AbT}}{J^{AbT}} MAC \left(j \frac{\hat{e}^{AbT}}{J^{AbT}} \right) \quad \text{and} \quad \hat{e}_{f,t} = J_{f,t} \frac{\hat{e}^{AbT}}{J^{AbT}}, \quad (10)$$

from which we can compute the final price of fossil fuels paid by firm f :

$$P_{f,t}^O = [1 + EC(\hat{e}_{f,t})] P_t^O. \quad (11)$$

Indeed, emissions costs (i.e., the carbon tax plus the abatement) act as a markup over the producer price, thus affecting the final demand for raw energy inputs.

To preserve the stock-flow consistency of the model, we assume that abatement costs incurred by firms are paid to a monopolist firm in the abatement sector and then distributed back to households, with the distribution proportional to their individual wealth (see Appendix A.8).

2.5. Growth

As the paper focuses on analyzing the long-term trends in the coupled climate-economic dynamics, it must also account for economic growth in the long run. To avoid overcomplicating the model, we introduce an exogenous growth process in the original MATRIX framework. Since labor and fossil fuels represent the sole exogenous inputs (i.e., energy and capital are endogenous as they are a combination of other factors of production), we assume that their productivity grows at a constant rate ζ^{growth} .¹⁵ In particular, given the CES production function:

$$Q_{f,t} = \left[\sum_{j=1}^J A_{j,f,t} (X_{j,f,t})^{\frac{\sigma_f-1}{\sigma_f}} \right]^{\frac{\sigma_f}{\sigma_f-1}}, \quad (12)$$

¹⁴ As for the carbon tax, we adopt this assumption to allow for its subsequent conversion into real-world monetary units (see Section 3).

¹⁵ In other words, we assume Harrod-neutral technical progress, which ensures a balanced growth path (Uzawa, 1961).

where $X_{j,f,t}$ is the quantity of input $j = 1, \dots, J$ employed by firm f at time t , $\sum_{j=1}^J A_{j,f,0} = 1$ are the factor shares, and σ_f is the Hicks elasticity of substitution, we update the factor shares as follow:

$$A_{j,f,t} = A_{j,f,t-1} (1 + \zeta^{growth})^{\frac{\sigma_f-1}{\sigma_f}}, \quad (13)$$

where j identifies both labor and fossil fuels. Accordingly, at each time t , firms internalize the expected growth of productivity (i.e., $\mathbb{E}_t[\zeta_{t+1}^{growth}] = \zeta^{growth}$) in their production decision for the subsequent period:

$$Q_{f,t+1}^* = (1 + \zeta^{growth}) Q_{f,t}^*, \quad (14)$$

where $Q_{f,t}^*$ is the desired production of firm f at time t (see Appendix A), leading to a proportional increase in the demand for inputs and promoting the accumulation of physical capital.

3. Calibration

In this work, we employ the parametrization of the MATRIX model presented in Turco et al. (2023), which provides a scale replica of the EA economy. Accordingly, the additional calibration effort regards the newly introduced parts, such as the climate modules, emissions, abatement functions, and damages. The calibration strategy is to follow real-world data whenever possible or rely on other studies when these are not available. In this Section, we provide a general overview of the new calibration focusing on the economic aspects of climate change.

Climate module and damage functions. Starting from the climate modules and damage functions, we retrieve most of the parameters from the supporting publications of the original models. Conversely, if specific coefficients or initial conditions are unavailable, we recover their values following the indications reported in the original studies.¹⁶ Appendix B provides a detailed description of the climate modules and a comprehensive list of the related parameters. At the same time, Section 2.3 illustrates the damage functions employed in this work and their sources.

CO₂ Emissions. Given the COVID-19 outbreak at the beginning of 2020, we set $t^* = 2019$ as a reference year for our analysis. We employ the historical emissions provided by the Our World in Data CO₂ and Greenhouse Gas Emissions dataset as an input of the climate module for the period between 1800 and 2020 and then forecast the future path of temperatures up to 2100 using the simulated emissions produced by the model.

Since we focus on the EA economy, we treat ROW emissions as exogenous and simulate their values by bootstrapping multiple time series from a vector autoregression model estimated on the log differences of global population, GDP per capita, and emission intensities.¹⁷ At the same time, we calibrate the consumption of fossil fuels and emission intensities of the model to replicate EA data. On the one hand, we follow Ciola et al. (2023) and Turco et al. (2023) to set the sectoral factor shares using the symmetric input-output tables at basic prices of Eurostat. In particular, we divide the 65 main activities of the dataset (European Classification of Economic Activities – NACE Rev. 2) between consumption (C) and capital (K) sectors using the relative weight of final consumption and investments on total demand as a proxy. Further, we identify the energy (E) and fossil fuel sectors with the category “Electricity, gas, steam and air conditioning” in the former case and with “Coke and refined petroleum products” and “Mining and quarrying” in the latter. Lastly, we compute sectoral factor shares by dividing the nominal expenditure on each intermediate input by total costs (see Table 3, second to fourth rows). On the other hand, we define

¹⁶ That essentially relates to the HECTOR model, where its initial conditions and a small number of parameters (related to ocean chemistry) depend on the resolution of a non-linear system of equations (Hartin et al., 2016).

¹⁷ See Appendix B for additional details.

Table 3
Production functions and emissions.

Sector		Consumption (C)	Capital (K)	Energy (E)	Source
Number of firms	\mathcal{N}^f	100	60	15	Ciola et al. (2023) and Turco et al. (2023)
Capital share	A_{K,f,t^*}	0.25	N/A	0.33	Eurostat: Symmetric input-output table at basic prices
Labor share	A_{N,f,t^*}	0.69	0.91	0.28	" "
Energy share	A_{E,f,t^*}	0.03	0.04	N/A	" "
Fossil fuel share	A_{O,f,t^*}	0.03	0.05	0.39	" "
Elasticity of substitution	σ_f	0.25	0.25	0.25	Ciola et al. (2023) and Turco et al. (2023)
Relative emission intensity	ε_{f,t^*}	1	0.46	1.40	Eurostat: Air emissions accounts by NACE Rev. 2 activity

the initial emission intensities of firms using their observed relative values, namely:

$$e_{f,t^*} = \frac{\varepsilon_{f,t^*} E_{t^*}}{\sum_{f=1}^{\mathcal{N}^f} \varepsilon_{f,t^*} O_{f,t^*}}, \tag{15}$$

where E_{t^*} are EA CO₂ emissions in 2019 (approx. 2.90 GtCO₂), O_{f,t^*} is the observed consumption of fossil fuels in the model, and ε_{f,t^*} are real-world relative emissions (see Table 3, last row). We compute the latter by converting EA sectoral emissions from NACE rev. 2 categories into the model ones (E, C, K) and then considering real-world sectoral expenditures on fossil fuels per unit of emission in terms of consumption firms.

Carbon tax and abatement. In Section 2, we design the (implicit) carbon tax $\tau_t^{CA^*}$ set by the government as a percentage τ_t^{CA} of the nominal expenditure on fossil fuels per unit of emission, namely:

$$\tau_t^{CA^*} = \frac{P_t^O}{e_{f^*,t^*}} \tau_t^{CA} = \frac{P_t^O O_{f^*,t^*}}{E_{f^*,t^*}} \tau_t^{CA} = \psi_{f^*,t^*}^{OE} \tau_t^{CA}. \tag{16}$$

Therefore, we can transpose model units into real-world monetary values by computing the conversion factor ψ_{f^*,t^*}^{OE} . In particular, given its predominant role in the model due to the high number of firms (see Table 3, first row), we use as a reference the consumption sector in 2019, which implies a value of $\psi_{f^*,t^*}^{OE} = 98$ euro per ton of CO₂ (EUR/tCO₂). Moreover, we assume that the government can adjust the tax τ_t^{CA} by one percentage point (i.e., $e^{CA} = 0.01$) in every period and test three different emissions reduction targets from the 2020 level: low ($\eta^{CA} = 0.25$), medium ($\eta^{CA} = 0.50$) and high ($\eta^{CA} = 0.75$). Lastly, to reduce the degree of subjectivity, we assume that the public sector evenly distributes the additional revenues in the available budget entries.

Moving to the AbT, Cline (2011) analyzes the abatement functions developed in three different models and computes their costs in percentage terms of GDP (Table 4). RICE 2008 and EMF 22 follows the well-known functional form developed by Nordhaus (2008). While the calibration of the former relies on the original work of Nordhaus (2008), the latter derives from its subsequent estimation on the results of the EMF 22 Climate Change Control Scenarios project (Clarke et al., 2009). Further, Ackerman and Bueno (2011) estimate a functional form reproducing the shape of the bottom-up MAC curve developed by McKinsey & Company (2009). Lastly, since we assume that abatement costs are a function of the nominal expenditure on fossil fuels, we convert the original curves by dividing them by the share of fossil fuels on total output ($v^O = 0.021$).

Fig. 3 provides a visual representation of their shapes: while all curves display similar costs for a high reduction objective (between 1.5% and 2% of real GDP), their marginal values are markedly different. Indeed, EMF 22 implies non-negligible initial costs, McKinsey follows an asymptotic behavior near the maximum, and RICE 2008 lies between the two. Lastly, we assume following Foramitti et al. (2021a) that the AbT is characterized by $J^{AbT} = 20$ steps up to a maximum percentage reduction of 80% ($\hat{e}^{AbT} = 0.8$, see Table 4). Moreover, we suppose firms revise their choices on average once a year, thus implying a quarterly switching probability $\theta^{AbT} = 0.25$.

4. Results and discussion

4.1. Climate assessment

We start by assessing climate change patterns by augmenting the MATRIX model with different carbon cycles currently employed in the literature (see Table 1). The goal is to construct a range of climate scenarios featuring low and high-temperature projections to analyze the economic impact of climate change.

Fig. 4 illustrates the coupled climate-economic dynamics generated by the model. The upper panel depicts the evolution of the simulated real GDP, which grows at a constant rate over time under the assumption of exogenous technical change. At the same time, quarterly global emissions follow real-world data between 1800 and 2020, while their trajectory derives from the simulated CO₂ paths after that year.

As stated before, the observed trends in the average temperature (Fig. 4, bottom panel) stem from various climate modules (i.e., DICE-2013R, C-ROADS, TCRE, WITCH, and HECTOR), which use as input the observed global emissions up to 2020 and the simulated time series from that year onwards. All frameworks closely replicate the temperature dynamics up to 2020 but, after that point, follow different trajectories despite the same macroeconomic and emission paths. The positive change in the average temperature compared to the preindustrial level ranges from nearly +1.2 °C (C-ROADS) to +2.2 °C (HECTOR) by 2050, and the gap between models widens by the end of the century, with +2 °C (C-ROADS) and +3.8 °C (TCRE) being the two extremes. Nevertheless, these trajectories are consistent with the IPCC scenarios (Byers et al., 2022; Calvin et al., 2023). In particular, HECTOR and TCRE models display the minimum distance from the baseline Shared Socioeconomic Pathways (SSP1 to SSP5), while C-ROADS and WITCH tend to underestimate the expected increase in the average temperature (see Table 5).

4.2. Economic effects of climate change

As global temperature rises, the economy suffers various climate-related damages that reduce firms' production capacity, expressed as a percentage reduction in labor productivity. As stated before, to evaluate the economic effects of climate change, we employ different climate damage functions developed in the current literature (DICE 1991, DICE 2013, DSK 2018, and RICE 1999). Further, we examine two types of climate shocks depending on whether the damage is homogeneous or heterogeneous across agents. Lastly, given the wide range of temperature projections generated by the different carbon cycles (see Fig. 4, bottom panel), we estimate the average temperature change and the resulting climate damages on three climate models – C-ROADS, DICE-2013R, and TCRE –, which represent the low-, medium-, and high-temperature scenarios, respectively.

Fig. 5 compares the estimated climate-induced GDP losses for the low-, medium-, and high-temperature scenarios (columns) using different damage functions (rows). The plots show the distribution of the values generated from 250 Monte Carlo runs, measured as the percentage deviation of real GDP from the BAU scenario (i.e., without damages) in 2100. The blue plots display the homogeneous climate shock case, while the red ones show the heterogeneous case. Table 6

Table 4
Abatement technology.

Total and marginal abatement cost functions (AC and MAC) relative to fossil fuel expenditure				
Name	AC	MAC	Parameters	Source
RICE 2008	$\frac{\alpha^{ABT}}{v^O} (\hat{e})^{\beta^{ABT}}$	$\frac{\alpha^{ABT}}{v^O} \beta^{ABT} (\hat{e})^{\beta^{ABT}-1}$	$\alpha^{ABT} = 0.028; \beta^{ABT} = 2.8$	Nordhaus (2008)
EMF 22	$\frac{\alpha^{ABT}}{v^O} (\hat{e})^{\beta^{ABT}}$	$\frac{\alpha^{ABT}}{v^O} \beta^{ABT} (\hat{e})^{\beta^{ABT}-1}$	$\alpha^{ABT} = 0.025; \beta^{ABT} = 1.28$	Clarke et al. (2009) and Cline (2011)
McKinsey	$\frac{\alpha^{ABT}}{v^O} \left[\log \left(\frac{\beta^{ABT}}{\beta^{ABT} - \hat{e}} \right) - \hat{e} \right]$	$\frac{\alpha^{ABT}}{v^O} \frac{\hat{e}}{\beta^{ABT} - \hat{e}}$	$\alpha^{ABT} = 8.6 \times 10^{-3}; \beta^{ABT} = 0.81$	Ackerman and Bueno (2011) and Cline (2011)
Other parameters				
Variable	Description	Value	Source	
v^O	Fossil fuel expenditure over total output	0.021	Eurostat: Symmetric input-output table at basic prices	
\hat{e}^{ABT}	Maximum potential abatement	0.80	Foramitti et al. (2021a)	
J^{ABT}	Number of abatement steps	20	Foramitti et al. (2021a)	
θ^{ABT}	Probability of new technology adoption	0.25	Authors' calibration	

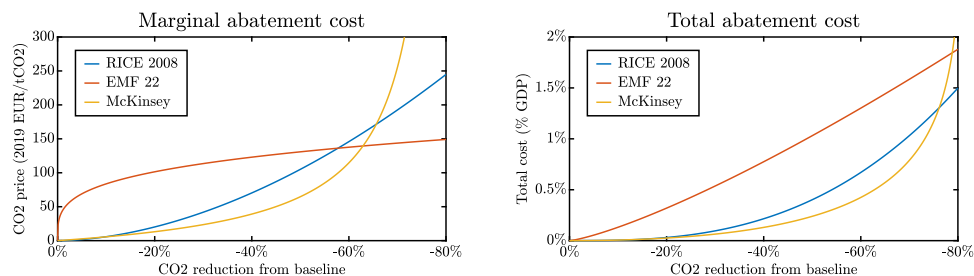


Fig. 3. Total and marginal abatement costs. *Note:* MAC curves in terms of 2019 EUR/tCO₂ (left panel) and total abatement costs in percentage terms of GDP (right panel) for different CO₂ emission reductions from the BAU level.

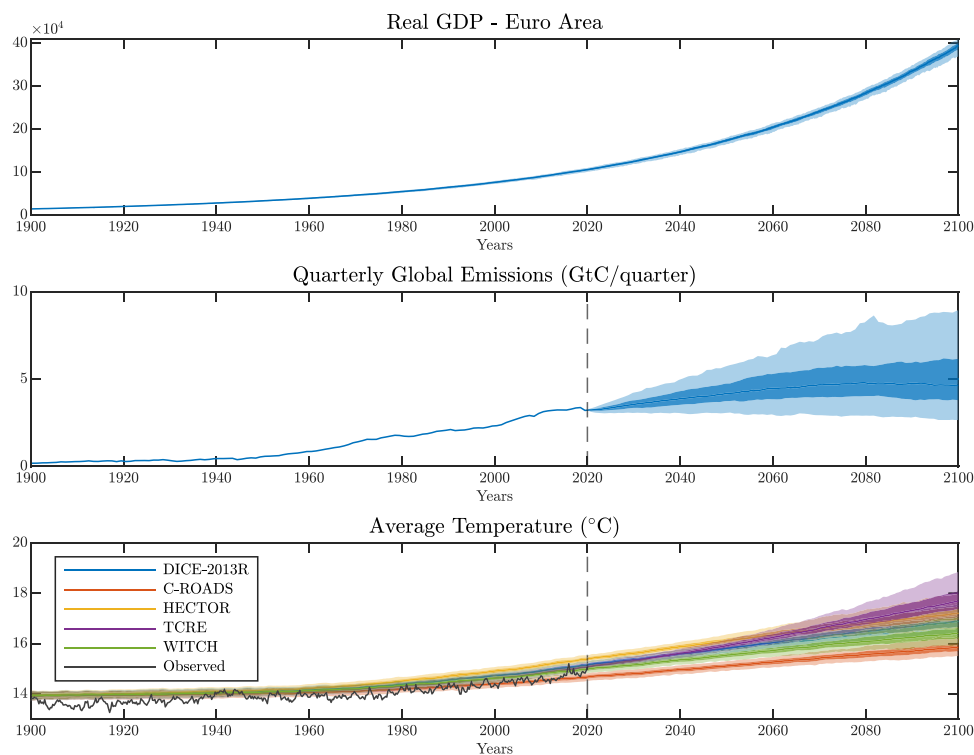


Fig. 4. Real GDP, global emissions, and average temperatures projections. *Note:* projections of real GDP (upper panel), global quarterly emissions (central panel), and average temperature (bottom panel) generated by the MATRIX model using different climate boxes. Medians (solid lines) and 90% confidence intervals (shaded areas) computed on 250 independent replicas of the model.

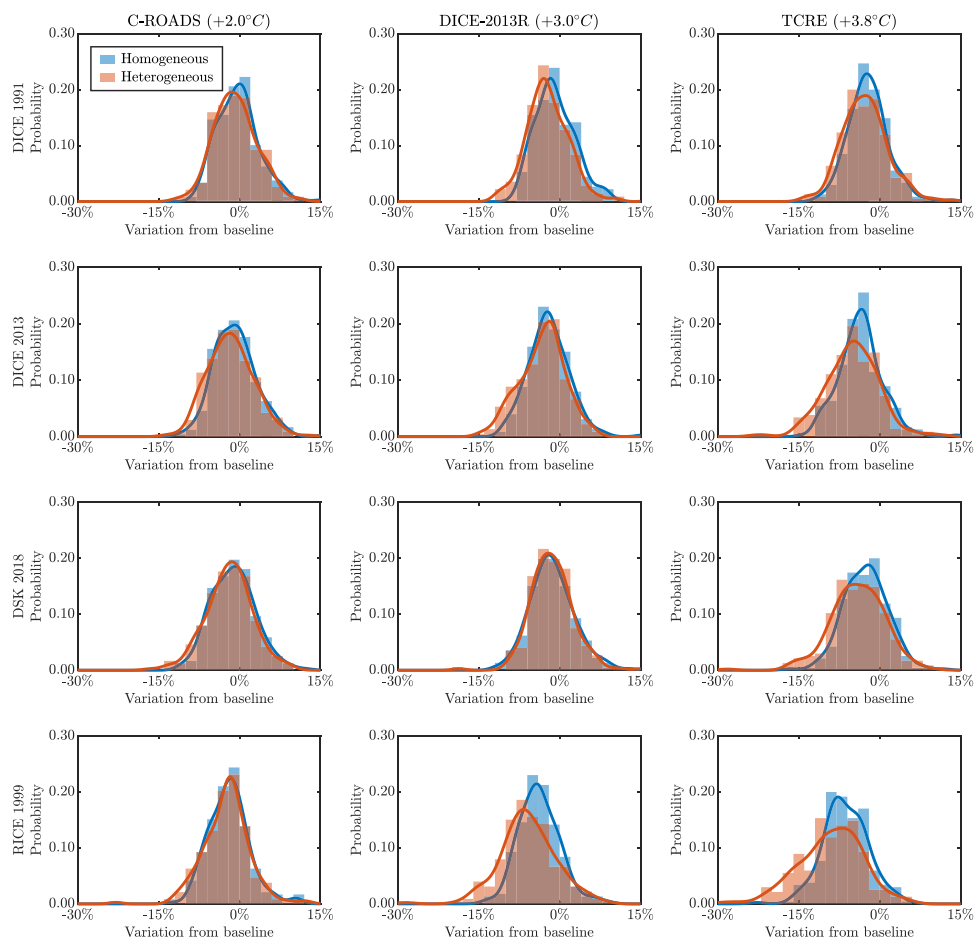


Fig. 5. Climate damages: real GDP loss in 2100. Note: real GDP loss from BAU in 2100 under heterogeneous and homogeneous shocks for low-, medium- and high-temperature scenarios using different damage functions. Results computed on 250 independent replicas of the model.

Table 5
Simulated temperature in climate modules and SSP scenarios.

	SSP1	SSP2	SSP3	SSP4	SSP5
DICE-2013R	0.09	0.14	0.14	0.08	0.25
C-ROADS	0.23	0.29	0.30	0.25	0.41
HECTOR	0.06	0.10	0.10	0.07	0.20
TCRE	0.07	0.09	0.08	0.08	0.18
WITCH	0.15	0.20	0.20	0.15	0.32

Note: root mean square error between temperature paths in selected climate modules (DICE-2013R, C-ROADS, TCRE, WITCH, and HECTOR) and baseline Shared Socioeconomic Pathways (SSP1 to SSP5) on the period 2020–2100.

provides a quantitative summary of the figures, indicating both the expected and realized losses resulting from the damage function.

Starting from homogeneous climate shocks, average GDP losses increase as temperatures rise, irrespective of the damage function under consideration. For example, according to Table 6, for RICE 1999, the realized reduction in real GDP at the end of the century rises from 2% under the low-temperature scenario to 6.4% under the high-temperature one. Similarly, for DSK 2018, GDP losses grow from 1.2% to 2.6%. The same trend holds also for heterogeneous climate shocks. However, in this case, not only does the average size of damages increase with the temperature, but also the dispersion of their distribution widens with global warming. Thus, in the presence of heterogeneous climate shocks, rising temperature affects both the magnitude and the volatility of losses from climate change. The enhanced volatility in economic damages also emerges in the wide gap between expected and realized outcomes in Table 6. While this gap is negligible under homogeneous shocks, it becomes significant in the other case. That means

that under heterogeneous climate shocks, the economy is more subject to business fluctuations and market disruptions resulting from adverse climate-related events than in the homogeneous case, experiencing, on average, a 50% increase in the impact of those shocks.

To better understand the reasons behind those different effects, it is worth exploring the climate impacts on other key macroeconomic variables. Table 7 compares the consequences of climate change on GDP deflator, real wage, and cumulative unemployment rate in 2100.¹⁸ On the one hand, results show that homogeneous climate damages act similarly to conventional supply shocks, leading to higher prices, lower real wages, and reduced employment. As expected, the magnitude of their effects increases with the temperature. On the other hand, heterogeneous climate shocks cause a further decline in output and employment, accompanied by falling prices and real wages. Although the economic losses stem from a reduction in firms' productivity, as in the homogeneous shock case, this situation is akin to a supply-induced demand shock.¹⁹ That is because the coordination failures

¹⁸ The cumulative unemployment rate is defined as the cumulative deviation from the baseline unemployment rate up to 2100.

¹⁹ The concept of a supply-induced demand shock, also referred to as a Keynesian supply shock, gained prominence within the context of the COVID-19 pandemic and the subsequent energy crisis (Guerrieri et al., 2022; Kharroubi and Smets, 2023). It consists of a negative supply shock capable of triggering a demand shortage, resulting in a contraction in output and employment that surpasses the magnitude of the initial supply shock. That typically occurs where strong sectoral complementarities exist, facilitating the transmission and amplification of the supply shock's effects from one sector to another.

Table 6
Climate damages: real GDP.

	C-ROADS (+2.0 °C)			DICE-2013R (+3.0 °C)			TCRE (+3.8 °C)		
	Expected	Realized Homog.	Heterog.	Expected	Realized Homog.	Heterog.	Expected	Realized Homog.	Heterog.
DICE 1991	-0.6%	-0.3%	-0.7%	-1.4%	-0.8%	-2.2%	-2.3%	-2.2%	-2.7%
DICE 2013	-1.0%	-0.9%	-1.6%	-2.4%	-2.1%	-3.3%	-3.9%	-3.6%	-5.1%
DSK 2018	-1.3%	-1.2%	-1.8%	-1.8%	-1.4%	-2.7%	-2.9%	-2.6%	-4.1%
RICE 1999	-1.7%	-2.0%	-2.4%	-4.0%	-3.8%	-5.8%	-6.6%	-6.4%	-9.1%

Note: average percentage deviation of real GDP from BAU for different climate boxes (C-ROADS, DICE-2013R, and TCRE), damage functions (DICE 1991, DICE 2013, DSK 2018, and RICE 1999), and shock types (homogeneous versus heterogeneous). Values computed on the last observation (year 2100) of 250 independent replicas of the model.

Table 7
Climate damages.

GDP deflator	C-ROADS (+2.0 °C)		DICE-2013R (+3.0 °C)		TCRE (+3.8 °C)	
	Homog.	Heterog.	Homog.	Heterog.	Homog.	Heterog.
DICE 1991	0.8%	0.6%	1.7%	0.7%	3.8%	-0.3%
DICE 2013	1.7%	0.4%	3.7%	-0.4%	5.8%	-1.1%
DSK 2018	1.9%	0.2%	2.3%	0.0%	3.8%	-0.5%
RICE 1999	3.2%	0.4%	5.5%	0.0%	10.3%	-1.6%
Real wage	C-ROADS (+2.0 °C)		DICE-2013R (+3.0 °C)		TCRE (+3.8 °C)	
	Homog.	Heterog.	Homog.	Heterog.	Homog.	Heterog.
DICE 1991	-0.6%	-1.3%	-1.2%	-2.9%	-2.1%	-4.6%
DICE 2013	-1.0%	-2.2%	-2.2%	-5.4%	-3.7%	-8.0%
DSK 2018	-1.4%	-3.3%	-1.9%	-4.9%	-2.9%	-7.3%
RICE 1999	-1.6%	-3.7%	-4.0%	-9.1%	-6.4%	-13%
Cumulative unemployment rate	C-ROADS (+2.0 °C)		DICE-2013R (+3.0 °C)		TCRE (+3.8 °C)	
	Homog.	Heterog.	Homog.	Heterog.	Homog.	Heterog.
DICE 1991	1.2%	4.9%	3%	12.5%	3.7%	22.3%
DICE 2013	2.1%	10.1%	4.8%	26.7%	8.8%	40.3%
DSK 2018	3.9%	14.9%	5.3%	23.2%	8.1%	35.9%
RICE 1999	2.3%	17.0%	10.6%	44.4%	16.2%	66.7%

Note: average percentage deviation of GDP deflator, real wage, and cumulative unemployment rate from BAU for different climate boxes (C-ROADS, DICE-2013R, and TCRE), damage functions (DICE 1991, DICE 2013, DSK 2018, and RICE 1999), and shock types (homogeneous vs. heterogeneous). Values computed on the last observation (year 2100) of 250 independent replicas of the model.

inherent in decentralized market interactions are exacerbated by heterogeneous climate shocks, resulting in a disordered impact on the economy. Faced with repeated supply bottlenecks, firms struggle to fulfill production requirements and need to reduce economic activity, leading to an increase in the unemployment rate, as shown in Table 7. A higher unemployment rate compresses the nominal wage with depressive effects on aggregate demand through the income channel, prices, and output. In contrast, the economy can better absorb homogeneous climate shocks since all agents react similarly to the same economic loss, allowing for more efficient coordination.

It is important to note that, when considering traditional homogeneous shocks, our findings are consistent with prior research on the effects of climate change that we use as a guide in the various damage function scenarios. However, they significantly diverge when we take into account heterogeneous shocks.

For a +3 °C warming, Nordhaus (1991) predicts net economic harm between 1% and 2% of total world output by 2050, while in an updated version (Nordhaus and Sutorc, 2013) estimate a GDP loss of 4% with a temperature increase of +3.8 °C by 2100. According to the regional variant (Nordhaus and Boyer, 2000), a +2.5 °C increase in global warming will cause a 2.8% reduction in Europe's GDP. Those results are consistent with our estimates produced using the DICE 1991, DICE 2013, and RICE 1999 damage functions, but only in the event of homogeneous climate shocks (see Table 6). Indeed, our work reveals that when heterogeneous climate shocks are taken into account, GDP

losses are substantially higher. That shows that standard IAMs founded on the representative agent hypothesis incur the danger of underestimating the economic impact of climate change (up to one-third under our estimates) by missing potential coordination failures resulting from real-financial linkages and decentralized market interactions.

As for the DSK2018, Lamperti et al. (2018) assess the impacts of disaggregated climate shocks in an agent-based IAM. Therefore, their projections can be directly compared to the heterogeneous scenario depicted in Table 6, though the outcomes are quite different. Based on an average temperature increase of +4.5 °C, the authors find that the average size of the damage fluctuates between 1% at the start and 5.4% at the end of the simulation. Regarding the actual impacts of these damages on the end-of-century GDP level, they find significant variations depending on the transmission channel of the climate shock under consideration, ranging from a 84.9% reduction through labor productivity to 13.5% through energy efficiency, 1.1% for inventories loss and 25.6% for capital stock, with additional harms when these shocks are combined. Despite the high values, a few warnings are in order. In contrast to the MATRIX model, the DSK framework features an endogenous growth process that has the potential to make climate shocks linger longer and possibly exacerbate their effects, particularly through channels related to labor productivity and capital stock.

4.3. Carbon tax and abatement

We assume that public authorities start implementing a carbon tax in 2020 and then dynamically adjust it depending on the wedge between actual and target CO₂ emissions. In other words, the government increases it if current emissions fall short of the target and reduces it in the opposite situation. As shown in Section 2.4, the carbon tax represents the implicit cost of emitting CO₂ in terms of fossil fuel consumption.²⁰ For this reason, we allow firms to invest in cost-effective emissions abatement technologies. In particular, they adopt a less polluting technology as long as its marginal cost is lower than the (implicit) emission price. At the same time, we also assess the effects of the carbon tax in the absence of any abatement technology as a robustness check. Indeed, the increase in the final cost of fossil fuels can also reduce their consumption and, consequently, CO₂ emissions. Nevertheless, the imperfect substitutability of this input with other production factors limits the extent of this type of emissions reduction strategy. In other words, this resembles a short-term situation in which firms do not have more efficient technologies at their disposition and try to substitute the relatively more expensive (and polluting) input with other (and cleaner) goods.

Fig. 6 shows the evolution of the carbon tax in terms of 2019 EUR per tonne of CO₂ for three different emissions reduction targets from the 2020 level: low (-25%), medium (-50%) and high (-75%). When firms can invest in an abatement technology, the tax converges to a stable value before the end of the century, and the implied price of

²⁰ Accordingly, we can compute its real-world counterpart by multiplying its value with the observed expenditure on fossil fuels per emitted ton of CO₂ (approx. 98 EUR/tCO₂ in 2019, see Section 3).

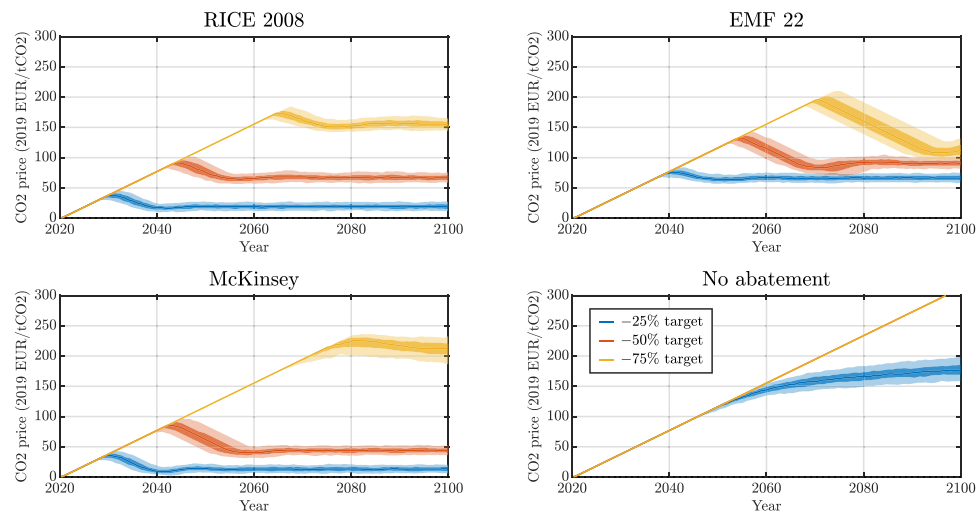


Fig. 6. Price of CO₂ emissions (2019 EUR/tCO₂) by emission target. *Note:* evolution of a carbon tax in 2019 euro per tonne of CO₂ (EUR/tCO₂) under different abatement technologies and emissions reduction targets: low (–25%), medium (–50%) and high (–75%). Median (solid line), 50% and 90% confidence intervals (shaded areas) computed on 250 independent replicas of the model.

Table 8
Carbon price, abatement technology and emissions targets.

Target	RICE 2008	EMF22	McKinsey	No abatement
–25%	18 ± 8	66 ± 8	13 ± 7	177 ± 20
–50%	67 ± 8	91 ± 9	44 ± 8	312 ± 0
–75%	155 ± 10	112 ± 17	212 ± 23	312 ± 0

Note: median plus 90% confidence intervals of a carbon tax in 2019 euro per tonne of CO₂ (EUR/tCO₂) under different abatement technologies and emissions reduction targets: low (–25%), medium (–50%) and high (–75%). Values computed on the last observation (year 2100) of 250 independent replicas of the model.

carbon is in line with existing studies (Clapp et al., 2009; Wagner et al., 2012; Hintermayer et al., 2020). In particular, a 25% reduction in CO₂ emissions requires a marginal cost of carbon between 15 and 70 EUR/tCO₂, while the achievement of the medium (–50%) and high (–75%) targets involves a value between 45 and 95 EUR/tCO₂ in the first case and between 110 and 210 EUR/tCO₂ in the second one (see Table 8). At the same time, the absence of an abatement technology allows the economy to reach only the least ambitious goal (i.e., –25% and with a marginal cost between 155 and 200 EUR/tCO₂), and the policy generates only a continuous but insufficient increase in the carbon price under the two alternative targets. In other words, given the limited substitutability of production factors in the short term, the growth in the price of fossil fuels does not sufficiently reduce their consumption and the related emissions (see Fig. 7). That highlights the importance of technological advancements and investments in emissions reduction since the straightforward substitution of fossil fuels with other production inputs is not feasible at affordable prices.²¹

An interesting aspect of the transition path is its non-linear behavior. After an initial period of positive growth, the carbon tax declines to a lower level in all the abatement technology scenarios (see Fig. 6). That is due to the slow adoption of new production techniques by firms, which need time to make the necessary investments and lag behind the choices made by the policymaker. Accordingly, when the economy reaches the emissions target (see Fig. 8), the carbon tax is far beyond the optimal level, firms continue investing in abatement technologies, and the government has to reduce it to keep the economy at the current (and desired) level of emissions. Moreover, the delay in

²¹ This result is even more significant since this version of the model does not allow firms to switch to greener energy sources as it assumes a single energy source.

Table 9
Real wage.

	Low (–25%)	Medium (–50%)	High (–75%)
RICE 2008	–0.5%	–1.1%	–1.9%
EMF 22	–1.3%	–1.9%	–2.2%
McKinsey	–0.3%	–0.8%	–1.8%
No abatement	–2.8%	–4.1%	–4.1%

Note: average percentage deviation of real wage under different abatement technologies and emissions reduction targets: low (–25%), medium (–50%) and high (–75%). Values computed on the last observation (year 2100) of 250 independent replicas of the model.

investments strongly depends on the shape of the abatement cost curve (see Fig. 9). High initial costs (as, for example, in the EMF 22 and no abatement scenarios) postpone (or completely prevent in extreme cases) the adoption of less polluting production techniques, instead favoring the substitution of fossil fuels with other production factors (see Fig. 7).

While changes in emission reduction targets do not significantly affect aggregate output, our analysis indicates that an escalation in carbon taxes leads to distributive consequences that adversely affect workers, who observe a decrease in the real wage (see Table 9). In practice, companies pass on the heightened production costs resulting from increased carbon taxes to their employees, thus diminishing their purchasing power.

Yet, these shifts in market income do not translate into significant variations in post-tax income distribution among individuals.²² Indeed, the redistributive measures implemented through government transfers play a pivotal role in restraining the growth of income and wealth inequality. Moreover, dividend redistribution from the abatement monopolist further mitigates disparities in individual incomes. These findings align with the “progressive revenues recycling” discussed in Konc et al. (2022). In the latter, the authors demonstrate that this type of recycling mechanism garners the most political support and may influence the long-term viability of the policy.

5. Concluding remarks

This work extends the MATRIX model (Ciola et al., 2023; Turco et al., 2023) to perform analyses akin to the IAMs literature, providing

²² We calculate it as variations in the Gini index and changes in income and wealth shares across quantiles.

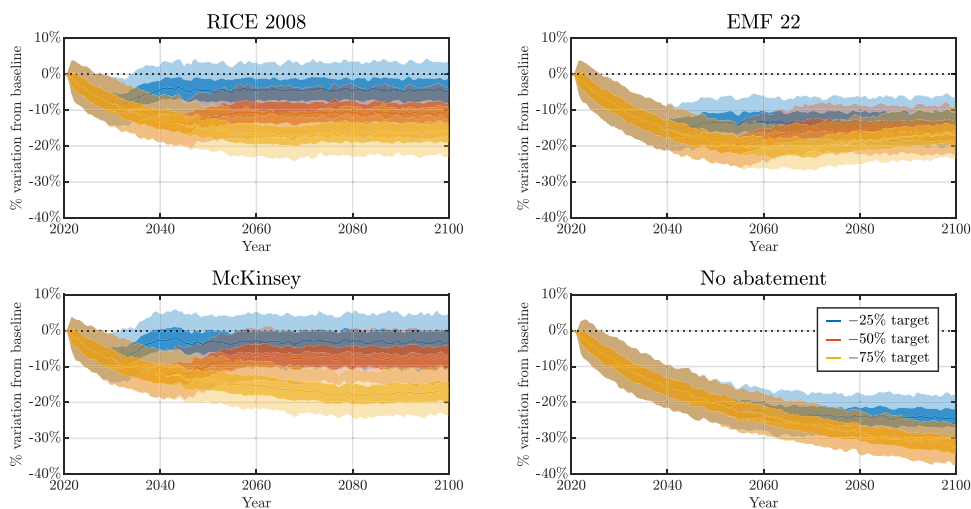


Fig. 7. Variation of fossil fuels consumption from baseline by emissions target. *Note:* evolution of fossil fuels consumption under different abatement technologies and emissions reduction targets: low (-25%), medium (-50%) and high (-75%). Median (solid line), 50% and 90% confidence intervals (shaded areas) computed on 250 independent replicas of the model.

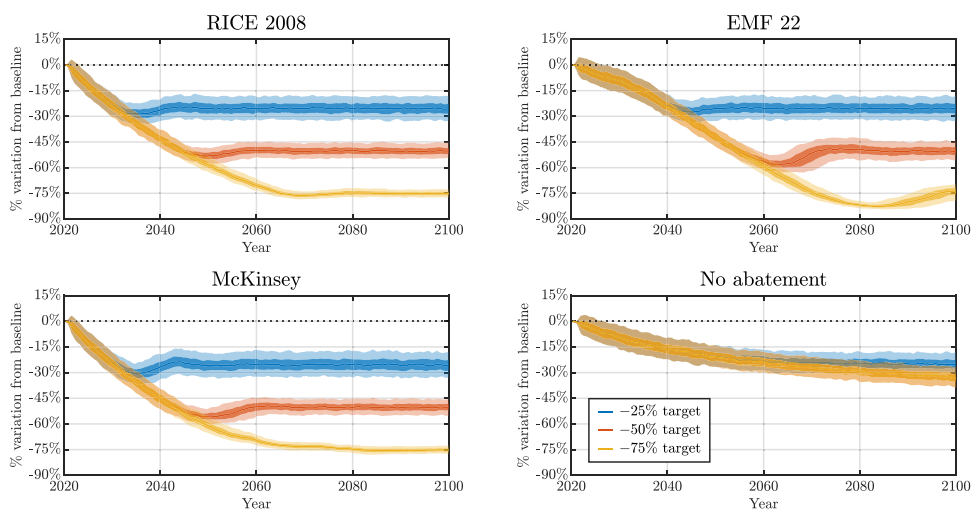


Fig. 8. Variation of CO₂ emissions from baseline by emissions target. *Note:* evolution of CO₂ emissions under different abatement technologies and emissions reduction targets: low (-25%), medium (-50%) and high (-75%). Median (solid line), 50% and 90% confidence intervals (shaded areas) computed on 250 independent replicas of the model.

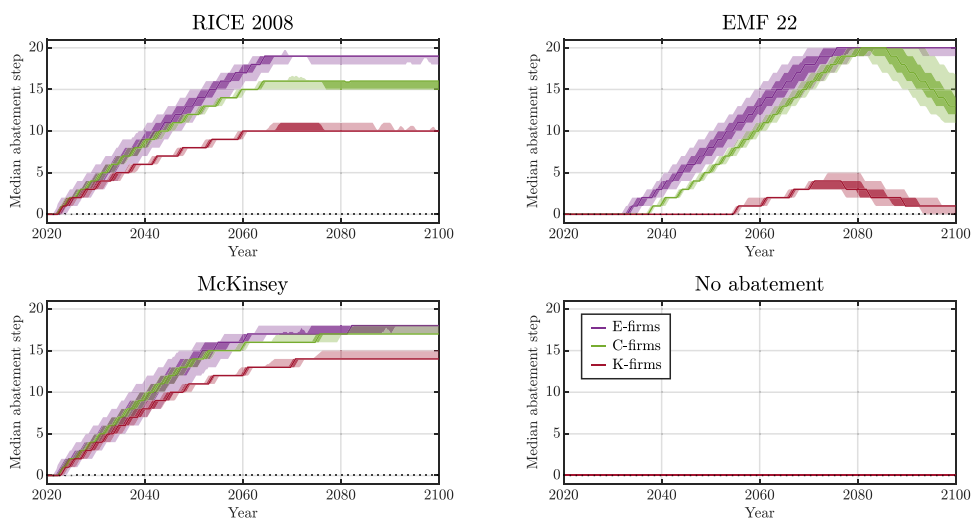


Fig. 9. Abatement step by sector. *Note:* median abatement step by sector under different abatement technologies and a high (-75%) emissions reduction target. Median (solid line), 50% and 90% confidence intervals (shaded areas) computed on 250 independent replicas of the model.

coupled dynamics for climate and economic systems. Given the substantial uncertainty surrounding relevant factors related to anthropogenic climate change (Pindyck, 2013), the modeling strategy entails an agnostic and flexible approach, which nests different carbon cycle modules, climate damages, and abatement cost functions. The model is calibrated to simulate the EA economy and evaluates the necessary carbon pricing to meet different climate objectives.

Our projections highlight a potential increase in the average temperature spanning from +2 °C to +3.8 °C at the end of the century. Selecting three representative temperature paths (low-, medium-, and high-), we then assess the effects of climate damages on the economy. We account for the uncertainty about their impacts by employing four different climate damage functions from the related literature. Moreover, we test them considering both homogeneous and heterogeneous effects on the population of agents.

On average, homogeneous climate damages may impact real GDP between 1.2% (low-temperature) to 3.7% (high-temperature), with significant differences between climate damage functions. Our results on climate damage are in line with the standard literature when we consider homogeneous shocks. Introducing heterogeneous shocks increases both their average size and dispersion, highlighting the loss of economic coordination in decentralized markets as a possible relevant factor in assessing climate change effects. Additionally, the characterization of the shock modifies accordingly, from a purely supply shock to a supply-induced demand shock, with falling prices and real wages.

We test a climate policy with various target shares of emission reductions for the EA economy, considering a carbon tax coupled with different abatement technologies. We show that in the absence of such a technology the carbon tax allows for reaching only the least ambitious climate objective with a higher carbon cost (between 155 and 200 EUR/tCO₂). On the contrary, when the abatement technology is available, all emission reduction objectives can be reached, resulting in carbon prices in line with previous studies. However, uncertainty about the abatement costs' functional shape leads to different adoption times, with higher initial costs significantly slowing the transition process. Finally, while changes to emission reduction targets have minimal impact on overall output, our analysis highlights that higher carbon taxes have negative effects on workers. This is evidenced by a decline in real wages, as companies transfer to their employees the higher production costs resulting from higher carbon taxes, thereby reducing their purchasing power. Despite these changes in market income, post-tax income distribution among individuals remains relatively unchanged. In the Matrix model, government transfers and dividend redistribution from the abatement monopolist are crucial in curbing the growth of income and wealth inequality.

Several theoretical and policy implications can be deduced from this framework. First, different combinations of IAMs' components can provide widely different scenarios, which require different levels of carbon pricing to reach the intended goals. An ensemble approach, as is standard in the climate assessment literature, can help to smooth the uncertainty embedded in these processes. Second, considering the complexity of the socioeconomic system can refine policy measures. Models with homogeneous (aggregate) climate damages – as standard IAMs grounded on the representative agent hypothesis – might underplay the resulting economic damage. Third, a reachable abatement technology is needed for the most ambitious climate targets, as well as affecting the speed of emission reductions. Related investments are, therefore, necessary alongside carbon pricing.

This work is subject to several limitations. Most notably, emission reduction relies mainly on a general abatement technology rather than considering alternative renewable energy options. Nevertheless, the energy transition will require a structural change in production processes, with huge investments in renewable energy production capacity and electrifying the economy. Accordingly, incorporating all those aspects into future versions of the model would allow investigating the economic and financial problems related to this process (see, among

others, Ponta et al., 2018; Safarzyńska et al., 2023; Di Domenico et al., 2023). At the same time, climate policy options can also be extended to include other channels, such as emission trading schemes, regulations, and subsidies for green technologies. That could also include other types of revenue recycling, which might bring different distributional effects (Konc et al., 2022). Additionally, as long as the model is calibrated on single states or economic areas, the global dimension of climate changes will be stylized, relying on exogenous paths for the evolution of the rest of the world's emissions.

Nevertheless, we show that the climate-extended MATRIX model could provide a solid base to develop all of these further extensions, themselves needed endeavors to assess climate change and the green transition in light of existing uncertainties and complexities.

CRedit authorship contribution statement

Daive Bazzana: Writing – review & editing, Writing – original draft, Visualization, Validation, Software, Methodology, Investigation, Formal analysis, Conceptualization. **Massimiliano Rizzati:** Validation, Software, Methodology, Investigation, Formal analysis, Conceptualization, Visualization, Writing – original draft, Writing – review & editing. **Emanuele Ciola:** Writing – review & editing, Writing – original draft, Visualization, Validation, Software, Methodology, Investigation, Formal analysis, Conceptualization. **Enrico Turco:** Writing – review & editing, Writing – original draft, Visualization, Validation, Methodology, Investigation, Formal analysis, Conceptualization, Software. **Sergio Vergalli:** Writing – review & editing, Visualization, Validation, Supervision, Software, Methodology, Investigation, Formal analysis, Conceptualization.

Appendix A. The MATRIX model

A.1. Overview

In this Appendix, we provide a brief exposition of the original MATRIX model's main components. For more details refer to the parental paper (Ciola et al., 2023; Turco et al., 2023).

The MATRIX model depicts an economy composed of heterogeneous agents. These include households, firms, banks, an exogenous fossil fuel sector, a central bank, and a government. Households ($h = 1, \dots, \mathcal{N}^H$) are divided between workers (\mathcal{N}^W), entrepreneurs (\mathcal{N}^E), and bankers (\mathcal{N}^B). Firms ($f = 1, \dots, \mathcal{N}^F$) belong to three different sectors: energy services (E), consumption goods (C), and capital goods (K). The banking sector consists of ($b = 1, \dots, \mathcal{N}^B$) banks. Entrepreneurs and bankers own respectively one firm and bank each.

Households. Households' income sources vary depending on their type and economic status. They receive a wage if employed; a dividend if they are an entrepreneur or banker of an active company; and a public transfer if their income falls below a certain level. Households buy consumption goods and save money in the form of bank deposits. Furthermore, firm and bank owners recapitalize their own companies in the event of a default.

Firms. Before beginning production, firms purchase the necessary inputs in decentralized markets. Subsequently, they update their net worth based on profits or losses and adjust their desired price, quantity, and related input demand for the following period. Because firms prepay for production factors, if the expected cash outflow exceeds internal funds, they borrow from banks to bridge the financing gap.

Banks. Banks hold deposits, lend to businesses in accordance with capital requirements, and purchase government bonds.

Government and central bank. The government collects income taxes from individuals and businesses, distributes transfers to low-income individuals and bails out failing banks. The deficit is funded by issuing new bonds, subject to a debt sustainability rule. The risk-free policy rate is set as an inertial Taylor rule by the central bank.

Matching protocol. The agents can observe only a portion of the market and interact with trading partners following a decentralized search and matching mechanism. Demand units visit supply units, with the ones offering larger amounts of goods at a lower price having higher chances to sell. It must be noticed that decentralized market interactions can result in unfilled demand or excess supply. Agents adapt their consumption and production plans due to matching frictions and changing economic conditions, which impact the macroeconomy. The latter is thus subject to cycles, fluctuations, and possibly recessions.

In the following, we present the sequence of events as well as a synthesis of the behavioral equations of the agents.

A.2. Sequence of events

The model follows this sequence of events (the novel parts compared to the original model are highlighted in italics):

1. Firms are already endowed with desired levels of production, selling prices, and input demands from the previous turn.²³
2. *If climate policy is binding, the government fixes or updates the carbon price level. Firms evaluate investment in abatement technology based on new information.*
3. Markets for production factors open:
 - i. Labor market: workers inelastically supply waged labor (up to one unit) to hiring firms, pay income taxes, and set their consumption budget;
 - ii. Fossil fuel market: firms purchase the energy input from the fossil fuel sector monopolist;
 - iii. Energy market: E-firms generate energy services by combining fossil fuel, labor, and capital goods. They sell them to C- and K-firms.
 - iv. Consumption goods market: C-firms combine capital stock, labor, fossil fuel, and energy services to produce the consumption goods. They sell it to households;
 - v. Capital goods market: K-firms supply capital goods to C- and E-firms employing labor, fossil fuel, and energy services;
4. Expected prices and quantities are updated. *These now include expected climate, abatement, and policy costs.*
5. Firms compute profits, their due taxes, the dividends to their owner, and the share of outstanding debt to the banks. *The accounting process of the firms now includes the costs borne for the abatement technology and the climate policy.*
6. Insolvent or illiquid firms that cannot be bailed by their owner's own resources default and new firms are initialized.
7. The firms set their new input demand for the next turn, given their expectations and resources, resorting eventually to the credit market. *This now accounts also for the expected climate-related costs.*
8. The Banks agents account for profits and NPL. Banks default procedure.
9. The government updates the tax rate and social transfers according to a fiscal sustainability rule.
10. The central bank fixes the policy rate given its Taylor rule.
11. *Climate module: firms emissions are updated. These act as an input to the climate module, that modifies the mean global temperature for the next turn or year.*
12. *Climate damages are computed and transmitted to the economy based on the previous turn variation in temperature.*

²³ The system is initialized at the perfect competition steady state solution at $t = 0$.

A.3. Households

The nominal income $Y_{h,t}$ of the households $h = 1, \dots, \mathcal{N}^W$ depends on their type:

$$Y_{h,t} = \begin{cases} W_t N_{w,t} & \text{for workers,} \\ DIV_{f,t} - REC_{f,t} & \text{for entrepreneurs,} \\ DIV_{b,t} - REC_{b,t} & \text{for bankers.} \end{cases} \quad (A.1)$$

Workers supply labor ($N_{w,t} \in [0, 1]$) in exchange for a uniform salary W_t that reflects market conditions and inflation expectations. Entrepreneurs and bankers get dividends, $DIV_{h,t}$ and sustain recapitalization costs, $REC_{h,t}$ if bankrupt. The household's consumption budget, $H_{h,t}^d$, is defined as the weighted sum between permanent income, $\tilde{Y}_{h,t}$,²⁴ and deposits:

$$H_{h,t}^d = \tilde{Y}_{h,t} + \chi D_{h,t}, \quad (A.2)$$

with χ being the propensity to consume out of financial wealth.

A.4. Firms

Firms agents – divided into three sectors (E, C, K) – set their desired price and quantity according to a learning mechanism based on market conditions and strategic interaction. In particular, they set the $\{P, Q\}$ combination by imitating the strategy of a target competitor,²⁵ if more profitable, or by exploring a neighbor of their current strategy. The firm f sets then a target s and updates its desired quantity and price $\{Q_{f,t+1}^*, P_{f,t+1}\}$:

$$Q_{f,t+1}^* = \begin{cases} \zeta^Q Q_{f,t}^* + (1 - \zeta^Q) Q_{s,t} & \text{if } \Pi_{s,t} \geq \Pi_{f,t}, \\ \zeta^Q Q_{f,t}^* + (1 - \zeta^Q) \hat{Q}_{f,t} & \text{otherwise,} \end{cases} \quad (A.3)$$

$$P_{f,t+1} = \begin{cases} \zeta^P P_{f,t} + (1 - \zeta^P) P_{s,t} & \text{if } \Pi_{s,t} \geq \Pi_{f,t}, \\ \zeta^P P_{f,t} + (1 - \zeta^P) \hat{P}_{f,t} & \text{otherwise,} \end{cases} \quad (A.4)$$

where $P_{s,t}$, $Q_{s,t}$ and $\Pi_{s,t}$ are, respectively the price, quantity, and profits of the target competitor s , while ζ^Q and ζ^P indicate the speed of adjustment of price and desired quantity. If the profits realized by the target firm s are greater than f 's, the latter are then smoothly adjusted towards them. Otherwise, the firm f explores a neighborhood of its current strategy, $\{\hat{Q}_{f,t}, \hat{P}_{f,t}\}$, by drawing a random number from a uniform distribution, the sign of which being positive (negative) in case of excess demand (supply).

Given $Q_{f,t+1}^*$, the desired production, and $\{\mathbb{E}_{f,t}[P_{j,t+1}]\}_{j=1}^n$, the expected input prices, each firm f sets the conditional input demand that minimizes its expected direct costs $\mathbb{E}_{f,t}[DC_{f,t+1}]$. The production technology is subject to a Constant Elasticity of Substitution (CES) and irreversible investments. Therefore, the cost minimization problem reads as:

$$\min_{\{X_{j,f,t+1}; \Delta X_{j,f,t+1}\}_{j=1}^J} \mathbb{E}_{f,t}[DC_{f,t+1}] = \sum_{j=1}^n \mathbb{E}_{f,t}[P_{j,t+1}] \Delta X_{j,f,t+1} \quad (A.5)$$

$$\text{s.t. } Q_{f,t+1}^* = \left[\sum_{j=1}^J A_{j,f,t+1} (X_{j,f,t+1})^{\rho_f} \right]^{\frac{1}{\rho_f}}, \quad (A.6)$$

$$X_{j,f,t+1} = \Delta X_{j,f,t+1} + (1 - \delta_j) X_{j,f,t}, \quad (A.7)$$

$$\Delta X_{j,f,t+1} \geq 0 \text{ when } j \text{ indicates physical capital,} \quad (A.8)$$

where $\Delta X_{j,f,t+1}$, δ_j , and $A_{j,f,t+1}$ are the additional input demand, the depreciation rate, and the factor share of input j , while ρ_f is the inputs

²⁴ The permanent income is set as a weighted average of current net income and past permanent income levels, updated by expected inflation.

²⁵ This is determined through a logit model computed as the difference between firms' relative production: $d_{f,s,t} = \left| \hat{y}_{f,t} - \hat{y}_{s,t} \right|$, where $\hat{y}_{f,t} \equiv \frac{P_{f,t} Q_{f,t} - \min(P_{f,t} Q_{f,t})}{\max(P_{f,t} Q_{f,t}) - \min(P_{f,t} Q_{f,t})}$.

substitution parameter. Following this problem, the nominal demand for an additional input is:

$$H_{j,f,t+1}^d = \mathbb{E}_{f,t} [P_{j,t+1}] \left[\left(\frac{A_{j,f,t+1} \psi_{f,t+1}}{\mathbb{E}_{f,t} [P_{j,t+1}]} \right)^{\sigma_f} Q_{f,t+1}^* - (1 - \delta_j) X_{j,f,t} \right] \quad \forall j = 1, \dots, J, \quad (\text{A.9})$$

where

$$\psi_{f,t+1} = \left[\sum_{j=1}^n (\mathbb{E}_{f,t} [P_{j,t+1}])^{1-\sigma_f} (A_{j,f,t+1})^{\sigma_f} \right]^{\frac{1}{1-\sigma_f}}, \quad (\text{A.10})$$

are the expected marginal costs.

If the expected direct costs are higher than internal liquidity, the firms try to borrow in a decentralized credit market. If credit rationing is present, firms set instead the optimal input demand that maximizes the attainable production. The firms seek then to satisfy their input demand in the different decentralized markets.

A.5. Banking sector

The banking sector provides credit to firms that need additional resources to purchase production inputs. The price of the loan depends upon the financial situation of the borrower-lender and on a systemic risk component, while its quantity on capital requirements. The interest rate $i_{b,f,t}$ on loans charged by bank b to the borrowing firm f at the time t is given by:

$$i_{b,f,t} = i_t^{CB} + \rho^B \frac{L_{f,t}}{NW_{f,t}} + \rho^B \left(1 - \frac{NWL_{b,t}}{\max_{s=1, \dots, N^B} NW_{s,t}} \right) + i_t^B \frac{NPL_{t-1}}{L_{t-1}}, \quad (\text{A.11})$$

where $\rho^B, \rho^B, i_t^B > 0$ are interest rate-related parameters. The cost of external finance is then increasing with the risk-free policy rate i_t^{CB} , the firm's leverage ratio, $L_{f,t}/NW_{f,t}$, and the non-performing loans ratio, NPL_{t-1}/L_{t-1} , while decreasing with the bank's net worth, $NW_{b,t}$.

In line with the Basel III international regulatory framework, banks must comply with macro-prudential capital requirements that define (i) the total amount of credit that they can extend and (ii) the maximum exposure to a single counterpart. That implies that borrowing firms might be unable to fully satisfy their financing needs, in which case they are forced to scale down the desired production and, subsequently, their input demand.

Banks must conform to macroprudential capital requirements, such as those under the Basel III international regulatory framework. That defines two constraints: first, the total amount of credit; second, the maximum exposure to a single counterpart. Borrowing firms may then be unable to fully satisfy their desired input demand and, thus, output level.

A.6. Central bank

The central bank sets the risk-free policy rate, i_t^{CB} , following a Taylor rule of the inertial type, that is:

$$i_t^{CB} = \rho^{CB} i_{t-1}^{CB} + (1 - \rho^{CB}) \max [0, r^* + p^* + \lambda^y (u^* - u_{t-1}) + \lambda^p (p_{C,t-1} - p^*)]. \quad (\text{A.12})$$

The central bank reacts to deviations in inflation and unemployment rates from their target levels, respectively p^* and u^* , given the steady-state interest rate r^* . The interest rate is slowly adjusted to avoid abrupt changes in firms' financing conditions, with ρ^{CB} defining the speed of adjustment (Castelnuovo, 2003).

A.7. Government

The government collects taxes (TAX_t) from the agents' income, distributes transfers (TRA_t) to low-income households, and provides liquidity of last resort (EXP_t) to failed banks. If in need, the government can issue additional bonds bought by the banking sector, and on which pays the risk-free policy rate (i_t^{CB}). Hence, public debt (B_t) evolves according to:

$$B_t = (1 + i_{t-1}^{CB}) B_{t-1} + TRA_t + EXP_t - TAX_t. \quad (\text{A.13})$$

The debt-to-GDP ratio dynamics can be written as:

$$b_{t+1} = \frac{1 + i_t^{CB}}{1 + g_t} b_t - f_{t+1}, \quad (\text{A.14})$$

where b_t is debt-to-GDP ratio, $f_t \equiv (TAX_t - TRA_t - EXP_t)/GDP_t$ is the primary budget-to-GDP, and g_t is the expected nominal growth rate of GDP. The government complies with a fiscal sustainability rule that prevents public debt from increasing indefinitely. Thus, the government adjusts gradually the current debt-to-GDP ratio to a target value b^* at a rate ρ^G :

$$b_{t+1} = b_t + \rho^G (b^* - b_t). \quad (\text{A.15})$$

(A.15) and (A.14) obtains the expected primary balance, that is:

$$-f_{t+1} = \rho^G b^* + (1 - \rho^G) \left[1 - \frac{1 + i_t^{CB}}{(1 + g_t)(1 - \rho^G)} \right] b_t. \quad (\text{A.16})$$

To comply with the expected primary balance, the government sets the tax rate, τ_t^{tax} . The share of social transfer over GDP, τ_t^{ra} , is fixed at a rate ψ^G . The latter can be increased only if:

$$\tau_t^{ra} = \max (\psi^G, -f_{t+1}), \quad (\text{A.17})$$

where τ_t^{ra} represents the share of social expenditures and ψ^G is the constant benchmark value, meaning that the expected primary balance guarantees enough fiscal space. The tax rate for the current period is then:

$$\tau_t^{tax} = \max (0, f_{t+1} + \tau_t^{ra}). \quad (\text{A.18})$$

If negative, the tax rate is set equal to zero, as consumer and firm subsidies are not considered in this version.

A.8. Stock-flow consistency

See Tables A.10 and A.11.

A.9. MATRIX model parameters

See Table A.12.

Appendix B. Climate boxes

This section presents the methodology employed to forecast ROW emissions and describes in details the alternative climate boxes tested in the paper.

B.1. Global emissions forecast

The Stochastic Impacts by Regression on Population, Affluence, and Technology (STIRPAT) framework (Dietz and Rosa, 1994, 1997; York et al., 2003; Liddle, 2015; Vélez-Henao and Font Vivanco, 2019) extends the standard IPAT equation (Ehrlich and Holdren, 1971, 1972; Commoner et al., 1972) by allowing for non-unitary elasticities between environmental impacts (I), population (P), affluence (A), and technology (T), namely:

$$I_t = a P_t^b A_t^c T_t^d Z_t, \quad (\text{B.1})$$

Table A.10
Aggregate balance sheet.

	Households	E-firms	C-firms	K-firms	Banks	Government	Central bank	Total
Deposits	$+D_h$	$+D_e$	$+D_c$	$+D_k$	$-D$			0
Capital		$+K_e$	$+K_c$					$+K$
Bonds					$+B_b$	$-B$	$+B_{cb}$	0
Loans		$-L_e$	$-L_c$	$-L_k$	$+L$			0
Reserves					$+H$		$-H$	0
Net worth	$-NW_h$	$-NW_e$	$-NW_c$	$-NW_k$	$-NW_b$	$-NW_g$		$-K$
Σ	0	0	0	0	0	0	0	0

Table A.11
Aggregate transaction flow matrix.

	Households	E-firms		C-firms		K-firms		Banks		Fossil fuel	Abatement	Government	Central bank	Σ
		CA	KA	CA	KA	CA	KA	CA	KA					
Consumption	$-C$	0	0	$+C$	0	0	0	0	0	0	0	0	0	0
Public Exp.	$+TRA$	0	0	0	0	0	0	$+EXP$	0	0	0	$-G$	0	0
Investment	0	0	$-I_e$	0	$-I_c$	$+I_k$	0	0	0	0	0	0	0	0
Abatement	$+Ab$	$-Ab_e$	0	$-Ab_c$	0	$-Ab_k$	0	0	0	0	$+Ab(-Ab)$	0	0	0
Energy	0	$+E$	0	$-E_c$	0	$-E_k$	0	0	0	0	0	0	0	0
Fossil fuel	$+(1-\eta_o)F$	$-F_e + \eta_o F$	0	$-F_c$	0	$-F_k$	0	0	0	$+F(-F)$	0	0	0	0
Wages	$+W$	$-W_e$	0	$-W_c$	0	$-W_k$	0	0	0	0	0	0	0	0
Taxes	$-T_h$	$-T_e$	0	$-T_c$	0	$-T_k$	0	$-T_b$	0	0	0	$+T$	0	0
Carbon taxes	0	$-CT_e$	0	$-CT_c$	0	$-CT_k$	0	0	0	0	0	$+CT$	0	0
Loan interests	0	$-iL_e$	0	$-iL_c$	0	$-iL_k$	0	$+iL$	0	0	0	0	0	0
Bonds interests	0	0	0	0	0	0	0	$+i^{CB}B_b$	0	0	0	$-i^{CB}B$	$+i^{CB}B_b$	0
Profits	$+DPr$	$-Pr_e$	$+UPr_e$	$-Pr_c$	$+UPr_c$	$-Pr_k$	$+UPr_k$	$-Pr_b$	$+UPr_b$	0	0	$+i^{CB}B_{cb}$	$-i^{CB}B_{cb}$	0
Stocks:														
Δ Deposits	$-\Delta D_h$	0	$-\Delta D_e$	0	$-\Delta D_c$	0	$-\Delta D_k$	0	$+\Delta D_b$	0	0	0	0	0
Δ Loans	0	0	$+\Delta L_e$	0	$+\Delta L_c$	0	$+\Delta L_k$	0	$-\Delta L_b$	0	0	0	0	0
Δ Bonds	0	0	0	0	0	0	0	0	$-\Delta B_b$	0	0	$+\Delta B$	$-\Delta B_{cb}$	0
Δ Reserves	0	0	0	0	0	0	0	0	$-\Delta H$	0	0	0	$+\Delta H$	0
Δ Total	0	0	0	0	0	0	0	0	0	0	0	0	0	0

or, in logarithm terms:

$$\log(I_t) = \log(a) + b \log(P_t) + c \log(A_t) + d \log(T_t) + \log(Z_t), \tag{B.2}$$

where a is a scale parameters, b , c , and d are the factor elasticities, and Z_t is a stochastic component.²⁶ In the case of CO₂ emissions, this formulation implies we can explicit them as a function of population (P), GDP per capita (A), and emission intensity (T), the latter measured as CO₂ emissions per unit of GDP.

Forecasting future global emissions thus requires an econometric framework that can model the interdependence between those factors, including potentially lagged effects. Accordingly, Vector Autoregression (VAR) can account for all these aspects: on the one hand, it introduces the lags of endogenous variables to control for delayed impacts; on the other hand, the variance-covariance matrix of innovations implicitly captures the contemporary interdependence between the variables (see Kilian and Lütkepohl, 2017).

We retrieve annual data on world population and real GDP (in constant 2015 US\$) from World Bank (2023), while Friedlingstein et al. (2022) provide a comprehensive dataset (The Global Carbon Budget 2022) on regional and global CO₂ emissions. Overall, our data span the period between 1965 and 2020, totaling 56 observations. After computing the GDP per capita (A) and emissions per unit of GDP (T), we test for unit roots in the time series (see Table B.13). Given the obtained results, we decide to use the first log difference of global emission intensity and GDP per capita while double differencing the logarithm of population to avoid underestimating the forecast variance.

We select the optimal lag order through the Akaike, Schwarz Bayesian, and Hannan-Quinn information criteria, which all point to one lag, and estimate the VAR(1) model:

$$y_t = \mu + B_1 y_{t-1} + \epsilon_t \quad \text{with} \quad y_t = \begin{bmatrix} \Delta^2 \log(P_t) \\ \Delta \log(A_t) \\ \Delta \log(T_t) \end{bmatrix}, \tag{B.3}$$

where μ is a vector of constants, B_1 is the matrix containing the coefficients of lagged effects, and $\epsilon_t \sim \mathcal{N}(0, \Sigma)$ is a vector of innovations with zero mean and variance-covariance matrix $\Sigma = B_0^{-1} B_0^{-1'}$, with B_0 being the (implicit) matrix capturing the contemporary interdependence between the endogenous variables (see Kilian and Lütkepohl, 2017).

We conclude by forecasting their values by bootstrapping 1000 independent replicas up to 2100 and then reconstructing the original time series (i.e., population, real GDP, and CO₂ emissions). Fig. B.10 compares the simulated paths (blue lines and shaded areas) with the baseline Shared Socioeconomic Pathways (SSP- Byers et al., 2022) from SSP1 to SSP5 (red lines). Our procedure covers most of the possible future evolutions of population and CO₂ emissions. Conversely, it tends to underestimate the expected growth of real GDP. Nevertheless, since the focus is on forecasting future emissions and our results match existing projections, we employ the simulated paths in the MATRIX model to predict the exogenous dynamics of ROW emissions.²⁷

B.2. Transient carbon response to cumulative emissions – TCRE

Climate literature identifies a direct linear relationship between emissions and temperature, often referred to as Transient Carbon Response to cumulative Emissions (TCRE) (Economides et al., 2018; Dietz and Venmans, 2019). This model simplifies the analysis in economic models but discounts eventual nonlinearities in climate change and is highly influenced by the parametrization value. In this version, the temperature anomaly evolves according to the following equation:

$$\Delta T_t = \Delta T_{t-1} + \eta_{TCRE} \zeta_{TCRE} E_t^W, \tag{B.4}$$

with η_{TCRE} being the initial pulse-adjustment timescale parameter, ζ_{TCRE} the TCRE parameter, and E_t^W global CO₂ emissions.

²⁷ In particular, we associate each simulated path to a specific random number generator seed of the MATRIX model.

²⁶ The standard IPAT equation implies: $a = b = c = d = Z_t = 1$.

Table A.12
MATRIX model: economy parameters.

Variable	Description	Value	Source
\mathcal{N}^W	Number of workers	1000	
β^C	Households discount rate	0.996	
ε	Households memory parameter	β^C	
χ	Marginal propensity to consume out of wealth	$1 - \beta^C$	
β^F	Firms discount rate	0.980	
μ^F	Firms dividend payout ratio	$1 - \beta^F$	
ρ^W	Wage stickiness	0.56	
θ^W	Insider–outsider bargaining power	0.51	
i^W	Inflation anchoring	0.67	
δ_N	labor depreciation rate	1	
\mathcal{N}^C	Number of C-firms	100	
$A_{N,C}$	Factor share capital (C-firms)	0.25	
$A_{K,C}$	Factor share labor (C-firms)	0.69	
$A_{E,C}$	Factor share energy (C-firms)	0.03	
$A_{O,C}$	Factor share natural resource (C-firms)	0.03	
δ_C	Consumption goods depreciation rate	1	
σ_C	Elasticity of substitution (C-firms)	0.25	
\mathcal{N}^E	Number of E-firms	15	
$A_{N,E}$	Factor share capital (E-firms)	0.28	
$A_{K,E}$	Factor share labor (E-firms)	0.33	
$A_{O,E}$	Factor share natural resource (E-firms)	0.39	
δ_E	Energy services depreciation rate	1	
σ_E	Elasticity of substitution (E-firms)	0.25	
\mathcal{N}^K	Number of K-firms	60	
$A_{N,K}$	Factor share labor (K-firms)	0.91	
$A_{E,K}$	Factor share energy (K-firms)	0.04	
$A_{O,K}$	Factor share natural resource (K-firms)	0.05	
δ_K	Depreciation rate of physical capital	0.05/4	
σ_K	Elasticity of substitution (K-firms)	0.25	
γ^{PQ}	Maximum size of price–quantity exploration	0.05	Ciola et al. (2023) and Turco et al. (2023)
ζ^Q	Speed of adjustment: quantity	0.75	
ζ^P	Speed of adjustment: price	0.75	
ω	Intensity of choice	10	
v^O	Foreign natural resource expenditure over GDP	0.021	
δ_O	Foreign natural resource depreciation rate	1	
η^O	Share of foreign natural resource going to E-firms	0.09	
\mathcal{N}^B	Number of banks	10	
γ^B	Capital adequacy ratio	0.08	
ω^B	Risk weighting	1	
κ^B	Maximum single exposure to borrowers	0.25	
ρ^B	Interest rate setting parameter: bank financial soundness	0.029/4	
ρ^B	Interest rate setting parameter: firm leverage	0.017/4	
i^B	Interest rate setting parameter: share of aggregate NPL	0.001/4	
θ^B	Share of loans repaid at each time-step	0.0125	
p^*	Inflation target	0.02/4	
u^*	Target unemployment rate	0.087	
r^*	Steady state real interest rate	$1/\beta^C - 1$	
λ^P	Monetary policy rule weights: inflation	1.41	
λ^u	Monetary policy rule weights: unemployment	0.11	
ρ^{CB}	Speed of adjustment of the monetary policy rule	0.85	
b^*	Target debt-GDP ratio	0.75	
ρ^G	Speed of adjustment to target debt-GDP ratio	0.007	
ψ^G	Share of social expenditures	0.094	
z^C	Maximum number of new partners (C-market)	0.25	
z^E	Maximum number of new partners (E-market)	4	
z^K	Maximum number of new partners (K-market)	4	
z^N	Maximum number of new partners (labor market)	10	
z^B	Maximum number of new partners (credit market)	0.2	

B.2.1. TCRE model parameters

See Table B.14.

B.3. Dynamic integrated climate-economy — DICE

We also consider a carbon cycle akin to the ones employed in the DICE 2013R model. That includes an ocean box and captures the interrelationships between the carbon concentrations and temperatures on the lower and upper parts of the ocean. The carbon stocks of the three reservoirs (atmosphere $C_{atm,t}$, upper ocean $C_{uo,t}$ and deep ocean $C_{lo,t}$) are updated by the exchanges between the three pools:

$$C_{atm,t} = f_{aa}C_{atm,t-1} + f_{ua}C_{uo,t-1} + E_{t-1}^W, \tag{B.5}$$

$$C_{uo,t} = f_{au}C_{atm,t-1} + f_{uu}C_{uo,t-1} + f_{lu}C_{lo,t-1}, \tag{B.6}$$

$$C_{lo,t} = f_{ul}C_{uo,t-1} + f_{ll}C_{lo,t-1}, \tag{B.7}$$

for f_{xy} with $x, y \in [a, u, l]$ denoting the share of the carbon in pool x flowing to the target pool y . The global temperature anomaly at the atmospheric level (ΔT_t) and the ocean one ($\Delta T_{o,t}$) are calculated as follows. First the radiative forcing (RF_t) is defined as:

$$RF_t = \eta \frac{\log \left[\frac{C_{atm,t-1}}{C_{atm,0}} \right]}{\log(2)}, \tag{B.8}$$

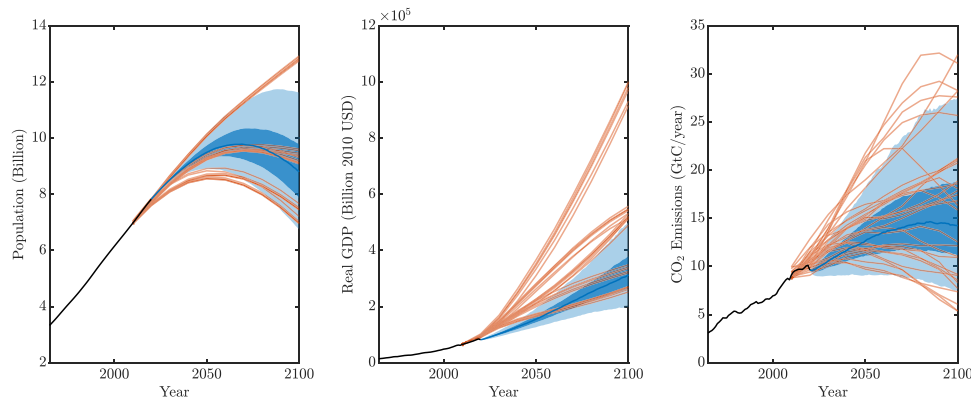


Fig. B.10. Simulated. *Note:* forecast of global population (left panel), real GDP (central panel), and CO₂ emissions (right panel) up to 2100. Median (blue solid line), 50% and 90% confidence intervals (blue shaded areas) computed on 1000 independent extractions. Red lines depict the official Shared Socioeconomic Pathways (SSP) from SSP1 to SSP5.

Table B.13

Augmented Dickey–Fuller test.

Variable	Constant	Constant and trend
$\log(P_t)$	0.1052	0.9994
$\log(A_t)$	0.3560	0.1127
$\log(T_t)$	0.9963	0.2288
$\Delta \log(P_t)$	0.9567	0.0140
$\Delta \log(A_t)$	3.06×10^{-5}	0.0002
$\Delta \log(T_t)$	2.16×10^{-6}	1.10×10^{-5}
$\Delta^2 \log(P_t)$	3.01×10^{-5}	0.0003

Note: p-values of Augmented Dickey–Fuller test with constant and constant plus trend on log and log difference (first and second) of population (P), GDP per capita (A), and emission intensity (T).

Table B.14

Climate box parameters, TCRC.

Variable	Description	Value	Source
η_{TCRC}	Transient carbon response to emissions	0.0019	Allan et al. (2021)
ζ_{TCRC}	Initial pulse-adjustment timescale	1	" "

with η being the forcing of equilibrium CO₂ doubling ($W\ m^{-2}$). Then,

$$\Delta T_t = \Delta T_{t-1} + c_1 \left[RF_t - \frac{\eta}{\lambda} \Delta T_{t-1} - c_3 (\Delta T_{t-1} - \Delta T_{o,t-1}) \right], \quad (B.9)$$

with c_1 being the climate equation coefficient for the upper-level ocean, λ the equilibrium temperature impact ($^{\circ}C$ per doubling CO₂), and c_3 the transfer coefficient from the upper to lower stratum. $\Delta T_{o,t}$ is defined as

$$\Delta T_{o,t} = \Delta T_{o,t-1} + c_4 (\Delta T_{t-1} - \Delta T_{o,t-1}), \quad (B.10)$$

with c_4 being the transfer coefficient for the lower level.

B.3.1. DICE model parameters

See Table B.15.

B.4. World induced technical change hybrid – WITCH

The World Induced Technical Change Hybrid (WITCH) model employs a carbon cycle derived from the DICE family of carbon cycles (Emmerling et al., 2016). Although similar to the one in the previous subsection, it is still included to test a different parametrization. The carbon atmosphere is set as:

$$C_{atm,t} = f_{aa} C_{atm,t-1} + f_{ua} C_{uo,t-1} + E_{t-1}^W, \quad (B.11)$$

with f_{xy} and $x, y \in [a, u, l]$ denoting the share of the carbon in pool x flowing to the target pool y . The upper ocean carbon pool is defined as:

$$C_{uo,t} = f_{au} C_{atm,t-1} + f_{uu} C_{uo,t-1} + f_{lu} C_{lo,t-1}, \quad (B.12)$$

whereas the lower ocean carbon is equal to:

$$C_{lo,t} = f_{ul} C_{uo,t-1} + f_{ll} C_{lo,t-1}. \quad (B.13)$$

The difference in GHG concentrations affects the change in the radiating factor:

$$RF_t = \eta \frac{\log \left[\frac{C_{atm,t-1}}{C_{atm,0}} \right]}{\log(2)}, \quad (B.14)$$

The atmosphere and ocean temperatures are updated accordingly:

$$\Delta T_t = \Delta T_{t-1} + \xi_1 \left[RF_{t-1} - \xi_2 \Delta T_{t-1} - \xi_3 (\Delta T_{t-1} - \Delta T_{o,t-1}) \right], \quad (B.15)$$

$$\Delta T_{o,t} = \Delta T_{o,t-1} + \xi_4 (\Delta T_{t-1} - \Delta T_{o,t-1}), \quad (B.16)$$

with ξ_1 being the lag parameter, ξ_2 the climate feedback parameter, ξ_3 the atmosphere–ocean exchange coefficient, and ξ_4 the ocean heat capacity.

B.4.1. WITCH model parameters

See Table B.16.

B.5. Climate rapid overview and decision support – C-ROADS

We now describe a climate module inspired by the Climate Rapid Overview And Decision Support (C-ROADS) model (Sterman et al., 2012). In this module, CO₂ in the atmosphere is determined by the interrelation between anthropogenic emissions and exchanges between an ocean and a land box.

B.5.1. Land

The Net Primary Production (NPP_t) absorbs carbon from the atmosphere:

$$NPP_t = NPP_0 \left[1 + \beta \log \left(\frac{C_{atm,t-1}}{C_{atm,0}} \right) \right] (1 - \beta_{T1} \Delta T_{t-1}), \quad (B.17)$$

where β_{T1} is a coefficient capturing the effect of the increase in mean surface temperature from the preindustrial level (ΔT_t) on NPP, and NPP_0 coincides with the preindustrial NPP. Part of the carbon can be stored or released from other stocks, namely the biosphere stock $C_{b,t}$ and the soil humus $C_{h,t}$. Therefore, other fluxes should be considered. These include the ones from the biosphere to the atmosphere, F_{ba} :

$$F_{ba} = \frac{C_{b,t-1}}{brt} (1 - hum), \quad (B.18)$$

where brt is the retention rate of carbon in the biosphere, and hum is the humification factor. Next is the flux from the soil to the atmosphere F_{ha} :

$$F_{ha} = \frac{C_{h,t-1}}{hrt}, \quad (B.19)$$

Table B.15

Climate box parameters: DICE.

Variable	Description	Value	Source
f_{ua}	Fraction of upper ocean carbon to atmosphere	0.267	Nordhaus (1993a)
f_{aa}	Fraction of staying atmosphere carbon	0.666	"
f_{uu}	Fraction of staying upper ocean carbon	0.610	"
f_{ns}	Fraction of atmosphere to upper ocean carbon	0.333	"
f_{lu}	Fraction of lower ocean carbon to upper ocean carbon	0.004	"
f_{ll}	Fraction of staying lower ocean carbon	0.995	"
f_{ul}	Fraction of upper ocean carbon to lower ocean	0.114	"
c_1	Lag parameter	0.226	"
η	Climate feedback parameter	2.9	"
c_2	Atmosphere ocean exchange-coefficient	0.44	"
c_4	Ocean heat capacity	0.02	"
λ	Scaling parameter	5.35	"
$C_{atm,0}$	Initial value CO ₂ atmosphere GtC	588	"
$C_{uo,0}$	Initial value CO ₂ upper ocean GtC	1350	"
$C_{lo,0}$	Initial value CO ₂ lower ocean GtC	10 000	"
$T_{uo,0}$	Initial value average temperature upper ocean °C	0.43	"
$T_{lo,0}$	Initial value average temperature lower ocean °C	0.06	"
T_0	Average temperature preindustrial level °C	14	"

Table B.16

Climate box parameters: WITCH.

Variable	Description	Value	Source
f_{ua}	Fraction of upper ocean carbon to atmosphere	0.04	Emmerling et al. (2016)
f_{aa}	Fraction of staying atmosphere carbon	0.88	"
f_{uu}	Fraction of staying upper ocean carbon	0.95	"
f_{ns}	Fraction of atmosphere to upper ocean carbon	0.12	"
f_{lu}	Fraction of lower ocean carbon to upper ocean carbon	0.00075	"
f_{ll}	Fraction of staying lower ocean carbon	0.999	"
f_{ul}	Fraction of upper ocean carbon to lower ocean	0.005	"
ξ_1	Lag parameter	0.226	"
ξ_2	Climate feedback parameter	1.36	"
ξ_3	Atmosphere ocean exchange-coefficient	0.31	"
ξ_4	Ocean heat capacity	0.05	"
λ	Scaling parameter	5.35	"
$C_{atm,0}$	Initial value CO ₂ atmosphere GtC	735	"
$C_{uo,0}$	Initial value CO ₂ upper ocean GtC	1000	"
$C_{lo,0}$	Initial value CO ₂ lower ocean GtC	10 000	"
T_0^o	Initial value average temperature upper ocean °C	1	"
T_0	Average temperature preindustrial level °C	14	"

with hrt being the retention rate for carbon into soil. Lastly, humification captures the flux from the biosphere to the soil layer through the flux F_{bh} :

$$F_{bh} = \frac{C_{b,t-1}}{brt} hum. \tag{B.20}$$

These fluxes affect the next period's atmospheric carbon stocks such that:

$$C_{atm,t} = C_{atm,t-1} + F_{ba} + F_{ha} - F_{ab}, \tag{B.21}$$

as well as the other stocks:

$$C_{b,t} = C_{b,t-1} + F_{ab} - F_{ba} - F_{bh}, \tag{B.22}$$

$$C_{h,t} = C_{h,t-1} + F_{bh} - F_{ha}. \tag{B.23}$$

B.5.2. Ocean

The carbon concentration in the atmosphere also depends on the exchanges with the oceans. These are modeled by a two-layer eddy diffusion box. The net carbon flux from mixed to deep ocean ($\Delta C_{md,t}$) depends on the difference in the carbon concentration in the two layers:

$$\Delta C_{md,t} = \kappa_{eddy} \frac{\frac{C_{m,t-1}}{d_m} - \frac{C_{d,t-1}}{d_d}}{\bar{d}_{md}}, \tag{B.24}$$

where $C_{md,t}$ is the mixed layer carbon concentration, d_x represent the thickness of the layer, \bar{d}_{md} is the average thickness and κ_{eddy} is a eddy diffusion parameter. The mixed layer carbon concentration depends on

the change both in atmospheric carbon concentration and temperature with respect to their preindustrial levels, and the Revelle factor ξ_t :

$$C_{m,t} = C_{m,0}(1 - \beta T_2 T_{m,t-1}) \left(\frac{C_{atm,t}}{C_{atm,0}} \right)^{1/\xi_t}, \tag{B.25}$$

The Revelle parameter (ξ_t) evolves over time following the atmospheric CO₂:

$$\xi_t = \xi_0 + \delta \log \left(\frac{C_{atm,t}}{C_{atm,0}} \right). \tag{B.26}$$

B.5.3. C-ROADS model parameters

See Table B.17.

B.6. HECTOR

In this section, we present a climate box inspired by the HECTOR model, which includes a three-module carbon cycle: atmosphere, land, and ocean (Hartin et al., 2015). In the climate box, any change in the atmospheric carbon depends on anthropogenic emissions (F_A) and the carbon fluxes between atmosphere–land (F_L) and atmosphere–ocean (F_O):

$$C_{atm,t} = C_{atm,t-1} + F_{A,t} - F_{L,t} - F_{O,t}. \tag{B.27}$$

As the emissions flux is such that $F_{A,t} = E_t^W$, we proceed now to describe the two other ones.

Table B.17
Climate box parameters: C-ROADS.

Variable	Description	Value	Source
C_o	CO ₂ ocean preindustrial level	10.237	Sterman et al. (2012)
NPP_0	Net primary production preindustrial level	85.177	"
β_c	Response of NPP to carbon	0.42	"
brt	Years carbon in bio retention	10.6	"
hrt	Years carbon in humus retention	27.8	"
hum	Humification factor	0.428	"
ξ_0	Revelle reference buffer factor	0.97	"
δ_c	Index for response of buffer to carbon concentration	3.92	"
κ_{eddy}	Eddy diffusion coefficient for circulation in ocean	4400	"
d_{mix}	Mixed ocean depth	100	"
d_{deep}	Deep ocean depth	3500	"
β_{T1}	Sensitivity of carbon uptake to temperature by land	-0.01	"
β_{T2}	Sensitivity of carbon uptake to temperature by ocean	0.003	"
c_1	Diffusion for atmospheric temperature	0.098	"
λ_c	Equilibrium climate sensitivity	2.9	"
c_3	Diffusion in deep oceans temperature equation	0.088	"
c_4	Sensitivity of atmospheric to deep ocean temperature	0.025	"
γ_{rf}	Radiative forcing coefficient	5.35	"
σ_{uplo}	Ocean heat capacity	11	"
$C_{atm,0}$	Initial value CO ₂ atmosphere GtC	590	"
$C_{uo,0}$	Initial value CO ₂ upper ocean GtC	1023.73	"
$C_{lo,0}$	Initial value CO ₂ lower ocean GtC	35 830	"
$C_{bio,0}$	Initial value CO ₂ biosphere GtC	902.87	"
$C_{hum,0}$	Initial value CO ₂ humus GtC	1013.5	"
$T_{uo,0}$	Initial value average temperature upper ocean	0.43	"
$T_{lo,0}$	Initial value average temperature lower ocean	0.06	"
$T_{i,0}$	Average temperature preindustrial level	14	"

B.6.1. Land

The land box is divided into three land layers (terrestrial vegetation, detritus, and soil), linked with each other and the atmosphere. The CO₂ absorption from the land layer $F_{L,t}$ depends on the difference between the net primary production (NPP) and the heterotrophic respiration of soil and detritus layers (RH_x , with $x \in [s, d]$):

$$F_{L,t} = NPP_t - RH_{d,t} - RH_{s,t}. \tag{B.28}$$

NPP_t is the net primary production representing how much carbon dioxide vegetation takes in during photosynthesis minus the quantity it releases with respiration:

$$NPP_t = NPP_0 \left[1 + \beta^{npp} \log \left(\frac{C_{atm,t-1}}{C_{atm,0}} \right) \right]. \tag{B.29}$$

According to (B.29), the net primary production depends on a carbon fertilization parameter β^{npp} and the change of the carbon stock in the atmosphere with respect to the preindustrial level. $RH_{y,t}$ denotes the heterotrophic respiration summed over user-specified boxes ($y \in [s, d]$ meaning soil and detritus) and evolves as follows:

$$RH_{y,t} = C_{y,t} f_{ry} Q_{10}^{T_{y,t}-1/10}. \tag{B.30}$$

The heterotrophic respiration in the two layers is a function of the carbon stock in detritus and soil ($C_{d,t}$ and $C_{s,t}$ respectively), the annual fraction of respiration carbon transferred to the detritus and soil layer (f_{rd} and f_{rs}), and Q_{10} , which represents the terrestrial respiration temperature response. Hence, the land carbon absorption is negatively affected by global warming, producing positive feedback dynamics between climate and carbon cycle (Sterman et al., 2012). The land carbon stocks dynamics are the result of changes in the fluxes between the three carbon land pools as follows:

$$C_{v,t} = NPP_t f_{nv} + C_{v,t-1}(1 - f_{vd} - f_{vs}), \tag{B.31}$$

$$C_{d,t} = C_{d,t-1}(1 - f_{ds}) + NPP_{t-1} f_{nd} + C_{v,t-1} f_{vd} - RH_{d,t}, \tag{B.32}$$

$$C_{s,t} = C_{s,t-1} + NPP_{t-1} f_{ns} + C_{v,t-1} f_{vs} + C_{d,t-1} f_{ds} - RH_{s,t}, \tag{B.33}$$

where C_v represents the carbon stock in vegetation, and f_{xy} is the annual fraction of carbon transferred from the upper layer x to the lower layer y , with $x \in [v, d]$ and $y \in [d, s]$.

B.6.2. Ocean

The ocean carbon cycle model extends the traditional box structure of Knox and McElroy (1984) following Lenton (2000). The ocean-atmosphere carbon flux is the sum of the ocean surface fluxes which depend upon the solubility of carbon within the two surface ocean boxes. According to Takahashi et al. (2009), each surface ocean box exchanges CO₂ emissions according to the atmosphere-ocean gradient of the partial pressure pCO_2 :

$$F_{i,t} = \Phi K h_{i,t} A r_i S c_{i,t}^{-1/2} U_{10}^2 \Delta p CO_2, \tag{B.34}$$

where Φ is a unit conversion parameter (Hartin et al., 2016), $K h_{i,t}$ represents the Henry's Law constant, $A r_i$ is the area of the surface layer i ($i = HL, LL$, meaning high and low latitude), whereas U_{10} and $S c_{i,t}$ are the average wind speed and the Schmidt number. The surface box temperatures are linearly dependent on the global atmospheric temperature and are initially set at 2 °C in the high latitudes and 22 °C in the low latitudes. This gradient in the ocean water temperature produces a flux of carbon into the cold high-latitude sea and a flow of carbon from the warm low-latitude sea.

To initialize the ocean component of the model, we take as fixed the physical flows of water between the ocean boxes, and we derive the initial level of carbon stocks consistent to reach a steady state. Following Lenton (2000), we assume a preindustrial atmosphere-ocean flow equal to 1 GtC per year that nets out in the steady state, with a positive outgassing from the waters at lower latitude (+1 GtC) and a negative one for the higher latitudes (-1 GtC). Alkaline levels alk_i in the two surface boxes are set to compel this assumption about flows. Alkaline levels, as well as the dissolved inorganic carbon ($DIC_{i,t}$), calculated from the atmospheric carbon, concur to solve the ocean chemistry subsystem (see Hartin et al., 2016, for the detailed carbonate chemistry equations), which defines the partial pressure $pCO_{2,i,t}$, the Schmidt parameter $S c_{i,t}$, and Henry's constant solubility parameter $K h_{i,t}$. At every turn, these are set to reflect the change in carbon differentials between the atmosphere and the ocean, affecting the flux $F_{O,t}$.

Within the ocean, the thermohaline circulation of water mass in the ocean generates a flux of carbon between the ocean boxes. This carbon flux from layer x to layer y in the ocean is positively affected by the

Table B.18
Climate box parameters: HECTOR.

Variable	Description	Value	Source
f_{ds}	Fraction of detritus carbon transferred to soil	0.6	Hartin et al. (2015)
f_{vs}	Fraction of vegetation carbon transferred to soil	0.001	"
f_{nd}	Fraction of NPP carbon transferred to detritus	0.6	"
f_{ns}	Fraction of NPP carbon transferred to soil	0.05	"
f_{nv}	Fraction of NPP carbon transferred to vegetation	0.35	"
f_{rd}	Fraction of respiration carbon transferred to detritus	0.25	"
f_{rs}	Fraction of respiration carbon transferred to soil	0.02	"
f_{vd}	Fraction of vegetation carbon transferred to detritus	0.034	"
$Q10$	Terrestrial respiration temperature response	2.45	"
β^{npp}	Carbon fertilization parameter	0.36	"
Φ	Unit conversion parameter	0.585	"
α_h	Henry constant solubility parameter of CO2	0.727	"
A_{ohs}	Fraction area of high latitude ocean	0.15	Sarmiento and Toggweiler (1984)
A_{ols}	Fraction area of low latitude ocean	0.85	Sarmiento and Toggweiler (1984)
U_h	Wind speed in ocean surface	6.7	Takahashi et al. (2009)
alk_{hl}	Alkalinity levels high latitude ocean box $\mu\text{mol/kg}$	2291×10^{-6}	Calibration
alk_{ll}	Alkalinity levels low latitude ocean box $\mu\text{mol/kg}$	2246×10^{-6}	Calibration
S	Ocean average salinity	34.5	Hartin et al. (2015)
$E_{LI}k_d$	Water mass exchange (low latitude to intermediate) $\text{m}^3 \text{s}^{-1}$	2.08×10^8	Lenton (2000) and Knox and McElroy (1984)
$E_{ID}k_{wi}$	Water mass exchange (intermediate to deep) $\text{m}^3 \text{s}^{-1}$	1.25×10^7	Lenton (2000) and Knox and McElroy (1984)
κ_{ols}	Thermohaline circulation $\text{m}^3 \text{s}^{-1}$	7.2×10^7	Hartin et al. (2015)
κ_{ohs}	High-latitude circulation $\text{m}^3 \text{s}^{-1}$	4.9×10^7	"
spy	Seconds per year	31 557 600	"
V_{ohs}	Volume of High latitude surface m^3	5.4×10^{15}	"
V_{ols}	Volume of Low latitude surface m^3	3.6×10^{16}	"
V_{ode}	Volume of intermediate ocean m^3	9.64×10^{17}	"
V_{oin}	Volume of deep ocean m^3	3.24×10^{17}	"
$C_{atm,0}$	Atmospheric carbon GtC	588.1	"
$C_{D,0}$	Initial Detritus carbon GtC	55.2941	Calibration
$C_{S,0}$	Initial Soil carbon GtC	1808.8235	Calibration
$C_{V,0}$	Initial Vegetation carbon GtC	500	Calibration
$C_{HL,0}$	Initial Surface high latitude ocean carbon GtC	138.72	Calibration
$C_{LL,0}$	Initial Surface low latitude ocean carbon GtC	723.15	Calibration
$C_{IO,0}$	Initial Intermediate ocean carbon GtC	8309.75	Calibration
$C_{DO,0}$	Initial Deep ocean carbon GtC	26 383.65	Calibration
NPP_0	Initial Net primary production GtC	50.0	Hartin et al. (2015)
$F_{L,0}$	Atmosphere–land steady state carbon flux GtC/y	0.0	Hartin et al. (2015)
$F_{O,0}$	Atmosphere–ocean steady state carbon flux GtC/y	0.0	Lenton (2000)
$T_{HL,0}$	High latitude surface ocean temperature $^\circ\text{C}$	2.0	Lenton (2000)
$T_{LL,0}$	Low latitude surface ocean temperature $^\circ\text{C}$	22.0	Lenton (2000)
λ_c	Equilibrium climate sensitivity	2.9	"
γ^{RF}	Radiative forcing coefficient	5.35	"
k_h	Ocean heat uptake efficiency	1.16	Hartin et al. (2015)

mass water exchanged ($Tr_{x \rightarrow y}$), the carbon stock in the two layers, and their volume (V) as follows:

$$F_{x \rightarrow y,t} = Tr_{x \rightarrow y} \left(\frac{C_{i,t}}{V_i} - \frac{C_{j,t}}{V_j} \right). \tag{B.35}$$

B.6.3. Global atmospheric temperature

The change in the surface global atmospheric mean temperature is calculated by:

$$\Delta T_i = \frac{\lambda}{1 + k_h} RF_i, \tag{B.36}$$

where λ is a climate feedback parameter, κ_h representing the ocean heat uptake efficiency and RF_i represents the total radiative forcing:

$$RF_i = \gamma^{RF} \log \left(\frac{C_{atm,t}}{C_{atm,0}} \right), \tag{B.37}$$

where γ^{RF} is a scaling parameter (Hartin et al., 2015).

B.6.4. HECTOR model parameters

See Table B.18.

References

Ackerman, F., Bueno, R., 2011. Use of McKinsey Abatement Cost Curves for Climate Economics Modeling. Working Paper WP-US-1102, SEI-U.S. URL: <https://EconPapers.repec.org/RePEc:ecb:ecbwp:2003232>.

Allan, R.P., Hawkins, E., Bellouin, N., Collins, B., 2021. IPCC, 2021: Summary for policymakers. In: Masson-Delmotte, V., Zhai, P., Pirani, A., Connors, S.L., Péan, C., Berger, S., Caud, N., Chen, Y., Goldfarb, L., Gomis, M.I., Huang, M., Leitzell, K., Lonnoy, E., Matthews, J.B.R., Maycock, T.K., Waterfield, T., Yelekçi, O., Yu, R., Zhou, B. (Eds.), Climate Change 2021: The Physical Science Basis. Contribution of Working Group I to the Sixth Assessment Report of the Intergovernmental Panel on Climate Change. Cambridge University Press, pp. 3–32. <http://dx.doi.org/10.1017/9781009157896.001>.

Balint, T., Lamperti, F., Mandel, A., Napoletano, M., Roventini, A., Sapio, A., 2017. Complexity and the economics of climate change: A survey and a look forward. *Ecol. Econom.* 138, 252–265. <http://dx.doi.org/10.1016/j.ecolecon.2017.03.032>.

Bosello, F., Carraro, C., Galeotti, M., 2001. The double dividend issue: Modeling strategies and empirical findings. *Environ. Dev. Econom.* 6, 9–45. <http://dx.doi.org/10.1017/S1355770X0100002X>.

Brown, T.C., Kroll, S., 2017. Avoiding an uncertain catastrophe: climate change mitigation under risk and wealth heterogeneity. *Clim. Change* 141, 155–166. <http://dx.doi.org/10.1007/s10584-016-1889-5>.

Burke, M., Hsiang, S.M., Miguel, E., 2015. Global non-linear effect of temperature on economic production. *Nature* 527, 235–239. <http://dx.doi.org/10.1038/nature15725>.

Byers, E., Krey, V., Kriegler, E., Riahi, K., Schaeffer, R., Kikstra, J., Lamboll, R., Nicholls, Z., Sandstad, M., Smith, C., van der Wijst, K., A. Khouradajie, A., Lecocq, F., Portugal-Pereira, J., Saheb, Y., Stromman, A., Winkler, H., Auer, C., Brutschin, E., Gidden, M., Hackstock, P., Harmsen, M., Huppmann, D., Kolp, P., Lepault, C., Lewis, J., Marangoni, G., Müller-Casseres, E., Skeie, R., Werning, M., Calvin, K., Forster, P., Guivarch, C., Hasegawa, T., Meinshausen, M., Peters, G., Rogelj, J., Samset, B., Steinberger, J., Tavoni, M., van Vuuren, D., 2022. AR6 scenarios database. <http://dx.doi.org/10.5281/ZENODO.5886911>.

Calvin, K., Dasgupta, D., Krinner, G., Mukherji, A., Thorne, P.W., Trisos, C., Romero, J., Aldunce, P., Barrett, K., Blanco, G., Cheung, W.W., Connors, S., Denton, F., Diongue-Niang, A., Dodman, D., Garschagen, M., Geden, O., Hayward, B., Jones, C., Jotzo, F., Krug, T., Lasco, R., Lee, Y.Y., Masson-Delmotte, V., Meinshausen, M.,

- Mintenbeck, K., Mokssit, A., Otto, F.E., Pathak, M., Pirani, A., Poloczanska, E., Pörtner, H.O., Revi, A., Roberts, D.C., Roy, J., Ruane, A.C., Skea, J., Shukla, P.R., Slade, R., Slangen, A., Sokona, Y., Sörensson, A.A., Tignor, M., van Vuuren, D., Wei, Y.M., Winkler, H., Zhai, P., Zommers, Z., Hourcade, J.C., Johnson, F.X., Pachauri, S., Simpson, N.P., Singh, C., Thomas, A., Totin, E., Alegría, A., Armour, K., Bednar-Friedl, B., Blok, K., Cissé, G., Dentener, F., Eriksen, S., Fischer, E., Garner, G., Guivarch, C., Haasnoot, M., Hansen, G., Hauser, M., Hawkins, E., Hermans, T., Kopp, R., Leprince-Ringuet, N., Lewis, J., Ley, D., Ludden, C., Niamir, L., Nicholls, Z., Some, S., Szopa, S., Trewin, B., van der Wijst, K.I., Winter, G., Witting, M., Birt, A., Ha, M., 2023. IPCC, 2023: Climate Change 2023: Synthesis Report. Contribution of Working Groups I, II and III to the Sixth Assessment Report of the Intergovernmental Panel on Climate Change [Core Writing Team, H. Lee and J. Romero (Eds.)]. Technical Report, IPCC, Geneva, Switzerland, <http://dx.doi.org/10.59327/ipcc/ar6-9789291691647>.
- Carraro, C., Galeotti, M., Gallo, M., 1996. Environmental taxation and unemployment: some evidence on the “double dividend hypothesis” in Europe. *J. Public Econom.* 62, 141–181. [http://dx.doi.org/10.1016/0047-2727\(96\)01577-0](http://dx.doi.org/10.1016/0047-2727(96)01577-0).
- Castelnuovo, E., 2003. Describing the Fed’s Conduct with Taylor Rules: Is Interest Rate Smoothing Important? Working Paper Series 232, European Central Bank, URL: <https://EconPapers.repec.org/RePEc:ecb:ecbwp:2003232>.
- Castro, J., Drews, S., Exadaktylos, F., Foramitti, J., Klein, F., Konc, T., Savin, I., van den Bergh, J., 2020. A review of agent-based modeling of climate-energy policy. *Wiley Interdiscip. Rev. Clim. Change* 11, e647. <http://dx.doi.org/10.1002/wcc.647>.
- Ciola, E., Turco, E., Gurgone, A., Bazzana, D., Vergalli, S., Menoncin, F., 2023. Enter the MATRIX model: a multi-agent model for transition risks with application to energy shocks. *J. Econom. Dynam. Control* 146, 104589. <http://dx.doi.org/10.1016/j.jedc.2022.104589>.
- Clapp, C., Karousakis, K., Buchner, B., Château, J., 2009. National and sectoral GHG mitigation potential. <http://dx.doi.org/10.1787/5k453xgppq9w-en>.
- Clarke, L., Edmonds, J., Krey, V., Richels, R., Rose, S., Tavoni, M., 2009. International climate policy architectures: Overview of the EMF 22 international scenarios. *Energy Econ.* 31, S64–S81. <http://dx.doi.org/10.1016/j.eneco.2009.10.013>.
- Cline, W.R., 2011. Carbon Abatement Costs and Climate Change Finance. *Policy Analyses in International Economics*; 96. Peterson Institute For International Economics, Washington, D.C.
- Commoner, B., Ehrlich, P.R., Holdren, J.P., 1972. Response. *Bull. Atom. Sci.* 28, 17–56. <http://dx.doi.org/10.1080/00963402.1972.11457931>.
- Czupryna, M., Franzke, C., Hokamp, S., Scheffran, J., 2020. An agent-based approach to integrated assessment modelling of climate change. *J. Artif. Soc. Soc. Simul.* 23. <http://dx.doi.org/10.18564/jasss.4325>.
- Dennig, F., Budolfson, M.B., Fleurbaey, M., Siebert, A., Socolow, R.H., 2015. Inequality, climate impacts on the future poor, and carbon prices. *Proc. Natl. Acad. Sci.* 112, 15827–15832. <http://dx.doi.org/10.1073/pnas.1513967112>.
- Di Domenico, L., Raberto, M., Safarzynska, K., 2023. Resource scarcity, circular economy and the energy rebound: A macro-evolutionary input-output model. *Energy Econ.* 128, 107155. <http://dx.doi.org/10.1016/j.eneco.2023.107155>.
- Dietz, T., Rosa, E.A., 1994. Rethinking the environmental impacts of population, affluence and technology. *Human Ecol. Rev.* 1, 277–300.
- Dietz, T., Rosa, E.A., 1997. Effects of population and affluence on CO2 emissions. *Proc. Natl. Acad. Sci.* 94, 175–179. <http://dx.doi.org/10.1073/pnas.94.1.175>.
- Dietz, S., Stern, N., 2015. Endogenous growth, convexity of damage and climate risk: How nordhaus’ framework supports deep cuts in carbon emissions. *Econ. J.* 125, 574–620. <http://dx.doi.org/10.1111/eoj.12188>.
- Dietz, S., Venmans, F., 2019. Cumulative carbon emissions and economic policy: In search of general principles. *J. Environ. Econom. Manage.* 96, 108–129. <http://dx.doi.org/10.1016/j.jeeem.2019.04.003>.
- Dosi, G., Napoletano, M., Roventini, A., Stiglitz, J.E., Treibich, T., 2020. Rational heuristics? Expectations and behaviors in evolving economies with heterogeneous interacting agents. *Econ. Inq.* 58, 1487–1516. <http://dx.doi.org/10.1111/ecin.12897>.
- Economides, G., Papandreou, A., Sartzetakis, E., Xepapadeas, A., 2018. The Economics of Climate Change. Bank of Greece, URL: https://www.bankofgreece.gr/Publications/BookTheEconomicsOfClimateChange_WebVersion.pdf.
- Ehrlich, P.R., Holdren, J.P., 1971. Impact of population growth. *Science* 171, 1212–1217. <http://dx.doi.org/10.1126/science.171.3977.1212>.
- Ehrlich, P.R., Holdren, J.P., 1972. Critique. *Bull. Atom. Sci.* 28, 16–27. <http://dx.doi.org/10.1080/00963402.1972.11457930>.
- Emmerling, J., Reis, L.A., Bevione, M., Berger, L., Bosetti, V., Carrara, S., Marangoni, G., Sferra, F., Tavoni, M., Witajewski-Baltvilks, J., Havllk, P., 2016. The WITCH 2016 model - documentation and implementation of the shared socioeconomic pathways. SSRN Electron. J. <http://dx.doi.org/10.2139/ssrn.2800970>.
- Farmer, J.D., Hepburn, C., Mealy, P., Teytelboym, A., 2015. A third wave in the economics of climate change. *Environ. Resour. Econom.* 62, 329–357. <http://dx.doi.org/10.1007/s10640-015-9965-2>.
- Foramitti, J., Savin, I., van den Bergh, J.C., 2021a. Emission tax vs. permit trading under bounded rationality and dynamic markets. *Energy Policy* 148, 112009. <http://dx.doi.org/10.1016/j.enpol.2020.112009>.
- Foramitti, J., Savin, I., van den Bergh, J.C., 2021b. Regulation at the source? Comparing upstream and downstream climate policies. *Technol. Forecast. Soc. Change* 172, 121060. <http://dx.doi.org/10.1016/j.techfore.2021.121060>.
- Friedlingstein, P., Jones, M.W., O’Sullivan, M., Andrew, R.M., Bakker, D.C.E., Hauck, J., Quéré, C.L., Peters, G.P., Peters, W., Pongratz, J., Sitoh, S., Canadell, J.G., Ciais, P., Jackson, R.B., Alin, S.R., Anthoni, P., Bates, N.R., Becker, M., Bellouin, N., Bopp, L., Chau, T.T.T., Chevallier, F., Chini, L.P., Cronin, M., Currie, K.I., Decharme, B., Djutchouang, L.M., Dou, X., Evans, W., Feely, R.A., Feng, L., Gasser, T., Giffillan, D., Gkritzalis, T., Grassi, G., Gregor, L., Gruber, N., Gürses, Özgür, Harris, I., Houghton, R.A., Hurtt, G.C., Iida, Y., Ilyina, T., Luijckx, I.T., Jain, A., Jones, S.D., Kato, E., Kennedy, D., Goldewijk, K.K., Knauer, J., Korsbakken, J.I., Körtzinger, A., Landschützer, P., Lauvset, S.K., Lefèvre, N., Lienert, S., Liu, J., Marland, G., McGuire, P.C., Melton, J.R., Munro, D.R., Nabel, J.E.M.S., Nakaoka, S.I., Niwa, Y., Ono, T., Pierrot, D., Poulter, B., Rehder, G., Resplandy, L., Robertson, E., Rödenbeck, C., Rosan, T.M., Schwinger, J., Schwingshackl, C., Séférian, R., Sutton, A.J., Sweeney, C., Tanhua, T., Tans, P.P., Tian, H., Tilbrook, B., Tubiello, F., van der Werf, G.R., Vuichard, N., Wada, C., Wanninkhof, R., Watson, A.J., Willis, D., Wiltshire, A.J., Yuan, W., Yue, C., Yue, X., Zaehle, S., Zeng, J., 2022. Global carbon budget 2021. *Earth Syst. Sci. Data* 14, 1917–2005. <http://dx.doi.org/10.5194/essd-14-1917-2022>.
- Gigerenzer, G., 2002. The adaptive toolbox. In: Gerd Gigerenzer, R.S. (Ed.), *Bounded Rationality*. The MIT Press, pp. 37–50. <http://dx.doi.org/10.7551/mitpress/1654.003.0005>, chapter The Adaptive Toolbox.
- Guerrieri, V., Lorenzoni, G., Straub, L., Werning, I., 2022. Macroeconomic implications of COVID-19: Can negative supply shocks cause demand shortages? *Amer. Econ. Rev.* 112, 1437–1474. <http://dx.doi.org/10.1257/aer.20201063>.
- Hafstead, M.A.C., Williams, R.C., 2020. Designing and evaluating a u.s. carbon tax adjustment mechanism to reduce emissions uncertainty. *Rev. Environ. Econom. Policy* 14, 95–113. <http://dx.doi.org/10.1093/reep/rez018>.
- Hartin, C.A., Bond-Lamberty, B., Patel, P., Mandra, A., 2016. Ocean acidification over the next three centuries using a simple global climate carbon-cycle model: projections and sensitivities. *Biogeosciences* 13, 4329–4342. <http://dx.doi.org/10.5194/bg-13-4329-2016>.
- Hartin, C.A., Patel, P., Schwarber, A., Link, R.P., Bond-Lamberty, B.P., 2015. A simple object-oriented and open-source model for scientific and policy analyses of the global climate system – hector v1.0. *Geosci. Model Dev.* 8, 939–955. <http://dx.doi.org/10.5194/gmd-8-939-2015>.
- Hintermayer, M., Schmidt, L., Zinke, J., 2020. On the Time-Dependency of MAC Curves and Its Implications for the EU ETS. *EWI Working Papers 2020-8*, Energiewirtschaftliches Institut an der Universität zu Köln (EWI), URL: https://ideas.repec.org/p/ris/ewikwn/2020_008.html.
- Kharroubi, E., Smets, F., 2023. Energy shocks as Keynesian supply shocks: implications for fiscal policy. URL: <https://www.bis.org/publ/work1120.htm>.
- Kilian, L., Lütkepohl, H., 2017. Structural vector autoregressive analysis. <http://dx.doi.org/10.1017/9781108164818>.
- Klenert, D., Mattauch, L., 2016. How to make a carbon tax reform progressive: The role of subsistence consumption. *Econ. Lett.* 138, 100–103. <http://dx.doi.org/10.1016/j.econlet.2015.11.019>.
- Knox, F., McElroy, M.B., 1984. Changes in atmospheric CO2: Influence of the marine biota at high latitude. *J. Geophys. Res.: Atmos.* 89, 4629–4637. <http://dx.doi.org/10.1029/jd089i03p04629>.
- Konc, T., Drews, S., Savin, I., van den Bergh, J.C., 2022. Co-dynamics of climate policy stringency and public support. *Global Environ. Change* 74, 102528. <http://dx.doi.org/10.1016/j.gloenvcha.2022.102528>.
- Lamperti, F., Dosi, G., Napoletano, M., Roventini, A., Sapio, A., 2018. Faraway, so close: Coupled climate and economic dynamics in an agent-based integrated assessment model. *Ecol. Econom.* 150, 315–339. <http://dx.doi.org/10.1016/j.ecolecon.2018.03.023>.
- Lamperti, F., Dosi, G., Napoletano, M., Roventini, A., Sapio, A., 2020. Climate change and green transitions in an agent-based integrated assessment model. *Technol. Forecast. Soc. Change* 153, 119806. <http://dx.doi.org/10.1016/j.techfore.2019.119806>.
- Lenton, T.M., 2000. Land and ocean carbon cycle feedback effects on global warming in a simple earth system model. *Tellus B: Chem. Phys. Meteorol.* 52 (1159), <http://dx.doi.org/10.3402/tellusb.v52i5.17097>.
- Liddle, B., 2015. What are the carbon emissions elasticities for income and population? Bridging STIRPAT and EKC via robust heterogeneous panel estimates. *Global Environ. Change* 31, 62–73. <http://dx.doi.org/10.1016/j.gloenvcha.2014.10.016>.
- Maestre-Andrés, S., Drews, S., Savin, I., van den Bergh, J., 2021. Carbon tax acceptability with information provision and mixed revenue uses. *Nature Commun.* 12. <http://dx.doi.org/10.1038/s41467-021-27380-8>.
- McKinsey & Company, 2009. Pathways to a Low-Carbon Economy: Version 2 of the Global Greenhouse Gas Abatement Cost Curve. McKinsey & Company, URL: https://www.mckinsey.com/~media/mckinsey/dotcom/client_service/sustainability/costcurvepdfs/pathways_lowcarbon_economy_version2.ashx.
- Montzka, S.A., Dlugokencky, E.J., Butler, J.H., 2011. Non-CO2 greenhouse gases and climate change. *Nature* 476, 43–50. <http://dx.doi.org/10.1038/nature10322>.
- Nordhaus, W.D., 1991. To slow or not to slow: The economics of the greenhouse effect. *Econ. J.* 101, 920–937. <http://dx.doi.org/10.2307/2233864>.
- Nordhaus, W.D., 1993a. Optimal greenhouse-gas reductions and tax policy in the “dice” model. *Am. Econ. Rev.* 83, 313–317, URL: <http://www.jstor.org/stable/2117683>.
- Nordhaus, W.D., 1993b. Rolling the ‘DICE’: an optimal transition path for controlling greenhouse gases. *Resour. Energy Econ.* 15, 27–50. [http://dx.doi.org/10.1016/0928-7655\(93\)90017-o](http://dx.doi.org/10.1016/0928-7655(93)90017-o).

- Nordhaus, W.D., 2008. *A Question of Balance*. Yale University Press, <http://dx.doi.org/10.12987/9780300165982>.
- Nordhaus, W., 2018. Evolution of modeling of the economics of global warming: changes in the dice model, 1992–2017. *Clim. Change* 148, 623–640. <http://dx.doi.org/10.1007/s10584-018-2218-y>.
- Nordhaus, W.D., Boyer, J., 2000. *Warming the World*. The MIT Press, <http://dx.doi.org/10.7551/mitpress/7158.001.0001>.
- Nordhaus, W.D., Sator, P., 2013. DICE 2013R: Introduction and Users Manual, second ed. URL: <https://yale.app.box.com/s/whlqcr7gtzdm4nxrnfhvap2hlzbeuvvm/file/1044222401276>.
- Palagi, E., Coronese, M., Lamperti, F., Roventini, A., 2022. Climate change and the nonlinear impact of precipitation anomalies on income inequality. In: *Proceedings of the National Academy of Sciences* 119. <http://dx.doi.org/10.1073/pnas.2203595119>.
- Parry, I.W.H., Bento, A.M., 2000. Tax deductions, environmental policy, and the “double dividend” hypothesis. *J. Environ. Econom. Manage.* 39, 67–96. <http://dx.doi.org/10.1006/jjeem.1999.1093>.
- Pindyck, R.S., 2013. Climate change policy: What do the models tell us? *J. Econ. Lit.* 51, 860–872. <http://dx.doi.org/10.1257/jel.51.3.860>.
- Ponta, L., Raberto, M., Teglio, A., Cincotti, S., 2018. An agent-based stock-flow consistent model of the sustainable transition in the energy sector. *Ecol. Econom.* 145, 274–300. <http://dx.doi.org/10.1016/j.ecolecon.2017.08.022>.
- Safarzyńska, K., Di Domenico, L., Raberto, M., 2023. The circular economy mitigates the material rebound due to investments in renewable energy. *J. Clean. Prod.* 402, 136753. <http://dx.doi.org/10.1016/j.jclepro.2023.136753>.
- Safarzyńska, K., van den Bergh, J.C.J.M., 2022. ABM-IAM: optimal climate policy under bounded rationality and multiple inequalities. *Environ. Res. Lett.* 17, 094022. <http://dx.doi.org/10.1088/1748-9326/ac8b25>.
- Sarmiento, J.L., Toggweiler, J.R., 1984. A new model for the role of the oceans in determining atmospheric p CO₂. *Nature* 308, 621–624. <http://dx.doi.org/10.1038/308621a0>.
- Savin, I., Creutzig, F., Filatova, T., Foramitti, J., Konc, T., Niamir, L., Safarzyńska, K., van den Bergh, J., 2023. Agent-based modeling to integrate elements from different disciplines for ambitious climate policy. *Wiley Interdiscip. Rev. Clim. Change* 14, 1–9. <http://dx.doi.org/10.1002/wcc.811>.
- Schmidt, M.G.W., Held, H., Kriegler, E., Lorenz, A., 2012. Climate policy under uncertain and heterogeneous climate damages. *Environ. Resour. Econom.* 54, 79–99. <http://dx.doi.org/10.1007/s10640-012-9582-2>.
- Sterman, J., Fiddaman, T., Franck, T., Jones, A., McCauley, S., Rice, P., Sawin, E., Siegel, L., 2012. Climate interactive: the c-ROADS climate policy model. *Syst. Dyn. Rev.* 28, 295–305. <http://dx.doi.org/10.1002/sdr.1474>.
- Takahashi, T., Sutherland, S.C., Wanninkhof, R., Sweeney, C., Feely, R.A., Chipman, D.W., Hales, B., Friederich, G., Chavez, F., Sabine, C., Watson, A., Bakker, D.C., Schuster, U., Metzl, N., Yoshikawa-Inoue, H., Ishii, M., Midorikawa, T., Nojiri, Y., Körtzinger, A., Steinhoff, T., Hoppema, M., Olafsson, J., Arnarson, T.S., Tilbrook, B., Johannessen, T., Olsen, A., Bellerby, R., Wong, C., Delille, B., Bates, N., d. Baar, H.J., 2009. Climatological mean and decadal change in surface ocean pCO₂, and net sea–air CO₂ flux over the global oceans. *Deep Sea Res. II: Top. Stud. Oceanogr.* 56, 554–577. <http://dx.doi.org/10.1016/j.dsr2.2008.12.009>.
- Turco, E., Bazzana, D., Rizzati, M., Ciola, E., Vergalli, S., 2023. Energy price shocks and stabilization policies in the MATRIX model. *Energy Policy* 177, 113567. <http://dx.doi.org/10.1016/j.enpol.2023.113567>.
- Tversky, A., Kahneman, D., 1974. Judgment under uncertainty: Heuristics and biases. *Science* 185, 1124–1131. <http://dx.doi.org/10.1126/science.185.4157.1124>.
- Uzawa, H., 1961. Neutral inventions and the stability of growth equilibrium. *Rev. Econ. Stud.* 28, 117–124. <http://dx.doi.org/10.2307/2295709>.
- Vélez-Henao, J.A., Font Vivanco, J.A., 2019. Technological change and the rebound effect in the STIRPAT model: A critical view. *Energy Policy* 129, 1372–1381. <http://dx.doi.org/10.1016/j.enpol.2019.03.044>.
- Wagner, F., Amann, M., Borken-Kleefeld, J., Cofala, J., Höglund-Isaksson, L., Purohit, P., Rafaj, P., Schöpp, W., Winiwarter, W., 2012. Sectoral marginal abatement cost curves: implications for mitigation pledges and air pollution co-benefits for annex i countries. *Sustain. Sci.* 7, 169–184. <http://dx.doi.org/10.1007/s11625-012-0167-3>.
- Weitzman, M.L., 2012. GHG targets as insurance against catastrophic climate damages. *J. Public Econ. Theory* 14, 221–244. <http://dx.doi.org/10.1111/j.1467-9779.2011.01539.x>.
- World Bank, 2023. World development indicators. Retrieved from <https://databank.worldbank.org/source/world-development-indicators>. 4th September 2023.
- York, R., Rosa, E.A., Dietz, T., 2003. STIRPAT, IPAT and ImPACT: analytic tools for unpacking the driving forces of environmental impacts. *Ecol. Econom.* 46, 351–365. [http://dx.doi.org/10.1016/s0921-8009\(03\)00188-5](http://dx.doi.org/10.1016/s0921-8009(03)00188-5).